lack of knowledge of the subsequent reaction of pip radicals with excess pip (i.e., total consumption of pip), and the relatively low [pip]₀/[TPPFeC]₀ ratios used to keep the autoreduction rate slow enough to follow by FT NMR. The relatively low sensitivity of NMR also did not permit a significant variation in [TPPFeCl]₀.

(41) C. E. Castro, personal communication.

(42) The experimental conditions were such that thermal effects from the light can be totally discounted.

(43) No attempt was made to fit the reduction rates to a rate law.

(44) L. A. Constant and D. G. Davis, *Anal. Chem.*, **47**, 2253 (1975).

(45) A. P. Tomilov, S. G. Mairanovskii, M. Y. Fioshin, and V. A. Smirnov in "Electrochemistry of Organic Compounds", Wiley, New York, N.Y., 1972, Chapter VIII.

(46) This >1 V barrier can be overcome in an outer-sphere electron transfer if one of the products (i.e., pip) is very short lived, i.e., <10⁻¹⁵ s (J. O'M. Bockris and A. K. N. Reddy, "Modern Electrochemistry", Plenum Press, New York, N.Y., 1970, Chapter 9). Such radicals, however, have been shown to have lifetimes ≥1 μs (ref 37).

(47) The authors are indebted to M. Gouterman for this suggestion.

(48) F. H. Westheimer, *Chem. Rev.*, **61**, 263 (1961).

(49) The isotope effect is not likely to be due to differential aggregation of the free pip, since lowering [pip]₀ by 30% maintained the same relative ratio of the pip/pip-*d*, autoreduction ratio.

(50) Attempts to obtain quantitative rate data for comparing NOHpip with NODpip in C²H₂Cl₂ at 25 °C were frustrated by the formation of a small but persistent amount of (TPPFe)₂O in spite of all attempts to remove both water and oxygen. The pyrrole-H peak of (TPPFe)₂O partially overlaps the same peak for the averaged (*S* = 0, *S* = 2) ferrous complexes, and interfered with quantitative integrations. Deconvolution repeatedly indicated a ~15–30% slower reduction with NODpip, but the large uncertainties placed the two rates within experimental error. The problem of the formation of (TPPFe)₂O was overcome by using degassed toluene-*d*₈ at 25 °C, where the dimer could not be detected. In this case, identical solutions reached 60% reduction in 163 min for NOHpip, and in 265 min for NODpip, confirming a retardation by deuterium of a factor of ~1.6.

(51) Mixed ligand complexes are formed when bases such as acetate, pyridine, or imidazole are added.

(52) S. Andreades and E. W. Zahnow, *J. Am. Chem. Soc.*, **91**, 4181 (1969).

Synthetic and Mechanistic Studies of the Reduction of α,β-Unsaturated Carbonyl Compounds by the Binuclear Cluster, NaHFe₂(CO)₈

James P. Collman,* **Richard G. Finke, Paul L. Matlock, Robert Wahren, Robert G. Komoto, and John I. Brauman***

Contribution from the Department of Chemistry, Stanford University, Stanford, California 94305. Received November 8, 1976

Abstract: A detailed synthetic and mechanistic study of the reactions of NaHFe₂(CO)₈ is presented including efficient preparations of Na₂Fe₂(CO)₈ and NaHFe₂(CO)₈. The use of NaHFe₂(CO)₈ for the mild, high-yield reductions of only the olefinic bond in α,β-unsaturated esters, ketones, aldehydes, amides, lactones, and nitriles is documented and these reductions are compared with other available methods. A mechanism for these reductions is presented. The key pieces of evidence for the mechanism, (a) a first order each in metal hydride and activated olefin, (b) isotopic labeling experiments demonstrating a reversible, regiospecific hydride addition step, and (c) a reasonably large, inverse isotope effect ($k_D/k_H = 3.5$), serve as diagnostics of the mechanism for reduction of activated olefins. We have considered plausible NaHFe₂(CO)₈ dissociation, fragmentation, or fragmentation–recombination mechanisms. The simplest interpretation of these results is that the active reagent in these reductions is binuclear NaHFe₂(CO)₈, although other possibilities are suggested and discussed. The above evidence and a complete reaction stoichiometry suggest that this mechanism involves concerted reversible and regiospecific NaHFe₂(CO)₈ addition to activated olefins such as RCH=CHCOR', to yield Na⁺(RCH₂CH(Fe₂(CO)₈)COR')⁻, followed by competing rate-determining steps of iron–iron bond cleavage or protonolysis affording Na⁺[RCH₂CH(Fe(CO)₄)COR']⁻ and RCH₂CH₂COR', respectively. This reduction mechanism using binuclear NaHFe₂(CO)₈ is compared with that of mononuclear NaHFe(CO)₄. The effect of ion pairing in these reductions, the PPh₃ and CO ligand substitution mechanism of NaHFe₂(CO)₈, as well as the acid-independent and acid-dependent mechanisms of NaHFe₂(CO)₈ decomposition are also presented.

Introduction

Transition metal carbonyl clusters[1] and their hydrides[2] have been known for many years, the first review on clusters appearing in 1965.[1g] Since that time, many studies probing the chemical composition and structural types,[1,4] the simple methods of synthesis,[1b] the relationship between the number of skeletal electrons and the structure,[3] and the fluxional behavior[5] of clusters have appeared. However, general, systematic, efficient synthetic routes for the preparation of clusters still do not exist.[6] Unfortunately, even less is known about the chemical reactivity[7,8,9] (especially the catalytic organometallic chemistry) and detailed reaction mechanisms[10] of clusters.

Our interest in binuclear and higher transition metal cluster compounds arises from the possibility that they will exhibit chemistry unknown to mononuclear homogeneous metal carbonyl compounds and may eventually serve as homogeneous models for reactions occurring on metal surfaces.[1b,11] Homogeneous mononuclear catalysts are unknown for many of the reactions catalyzed by heterogeneous catalysts, such as the

Fischer–Tropsch reaction[12] or reactions involving carbon-hydrogen[13] or carbon–carbon[14] bond activation. These and similar structure-sensitive[15] reactions may require two or more adjacent metals, a feature present in heterogeneous and homogeneous cluster catalysts but absent in mononuclear homogeneous catalysts. However, certain inherent properties and side reactions of clusters will severely thwart the development of their chemistry. In particular, metal–metal bonds are often weak,[16] imparting limited thermal stability to first- and second-row clusters. Photolysis usually results in metal–metal bond cleavage.[17] Homolysis[18] and disproportion[16] of clusters can occur giving rise to mononuclear and other fragments. Although not well studied, oxidation or reduction of clusters[1b,16] generally gives metal–metal bond cleavage. Clusters are often unstable under high CO pressure,[1b,1e] cleaving to mononuclear compounds. Added ligands, such as phosphines, may result in ligand substitution or metal–metal bond cleavage.[1b,1e,10] Indeed, the present study has demonstrated most of these side reactions in this simple binuclear cluster, NaH-
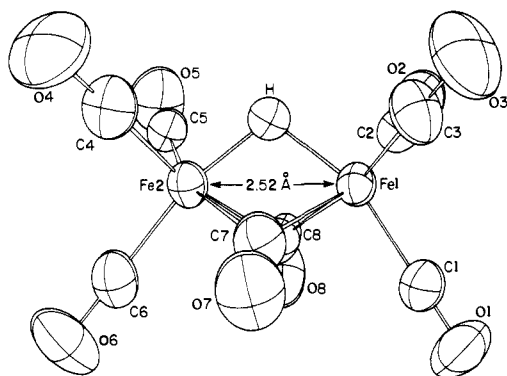
Figure 1. ORTEP plot of the $HFe_2(CO)_8^-$ anion.[24]

$Fe_2(CO)_8$. Thus the establishment of the reactive species in a "cluster" reaction is a very important but difficult task.[19]

Previously we reported[21] preliminary synthetic and mechanistic results on the reduction of the olefinic double bond in α,β-unsaturated carbonyl compounds by the binuclear cluster hydride, $NaHFe_2(CO)_8$. Herein, we report full synthetic and mechanistic details of this reduction reaction. We also describe the $NaHFe_2(CO)_8$ decomposition mechanisms, its ligand substitution mechanism, and its spectroscopic properties. The reaction of the monoiron hydride, $NaHFe(CO)_4$, with α,β-unsaturated carbonyl compounds has also been briefly examined, so that $NaHFe(CO)_4$ reductions can be compared and contrasted to those employing $NaHFe_2(CO)_8$.

Results

Preparation and Physical Properties of $NaHFe_2(CO)_8$. The binuclear hydride, $NaHFe_2(CO)_8$ (1), is prepared in a quantitative, two-step, one-flask reaction from $Na_2Fe(CO)_4$-1.5dioxane (11).[22] The parent dianion of $NaHFe_2(CO)_8$, $Na_2Fe_2(CO)_8$ (111), is prepared by condensation of $Na_2Fe(CO)_4$-1.5dioxane with $Fe(CO)_5$ (eq 1) in THF.

$$Na_2Fe(CO)_4\text{-}1.5dioxane + Fe(CO)_5$$
$$11$$
$$\xrightarrow{THF} Na_2Fe_2(CO)_8 \cdot 4THF + CO \quad (1)$$
$$111$$
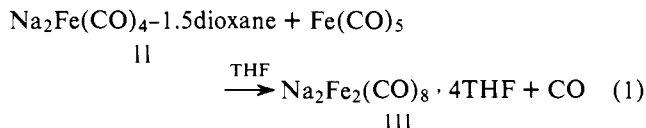
The $Na_2Fe_2(CO)_8$ is obtained as an orange precipitate and contains approximately 4 equiv of THF solvate. This solvate can be removed by evacuation with heating to yield $Na_2Fe_2(CO)_8$ as a bright yellow powder.

Solutions of $NaHFe_2(CO)_8$ are readily obtained by the addition of acetic acid to a stirred slurry of $Na_2Fe_2(CO)_8$ in THF:

$$Na_2Fe_2(CO)_8 + HOAc \xrightarrow{THF} NaHFe_2(CO)_8 + NaOAc$$
$$(2)$$
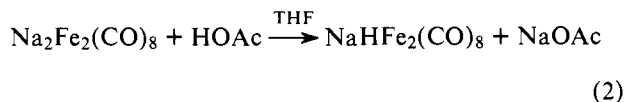
The sodium acetate formed causes a thickening of the THF solutions. This thickening limits the concentration of THF solutions of $NaHFe_2(CO)_8$ to about 0.2 M. The NaOAc can be removed by centrifugation, yielding a homogeneous, red-brown solution. The NaOAc does not hinder synthetic reductions, but it was removed for kinetic measurements.

The structure of $(HFe_2(CO)_8)^-$, isolated as the PPN^+ salt,[23] has been determined by x-ray diffraction by Chin and Bau[24] (Figure 1). The structure shows two bridging carbonyls and a bridging hydride. The bridging hydride was located using low angle data. The iron–iron bond distance in $HFe_2(CO)_8^-$, 2.521 (1) Å, is considerably shorter than the iron–iron single bond[25] in $Fe_2(CO)_8^{2-}$ of 2.787 (2) Å. If a bridging carbonyl is substituted for the bridging hydride in $HFe_2(CO)_8^-$, isostructural

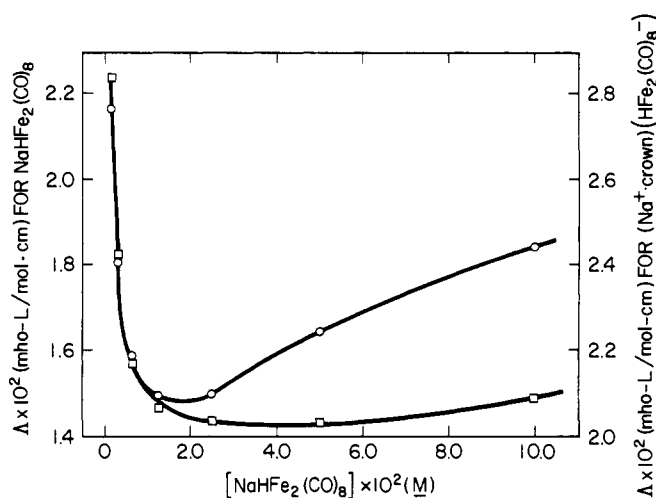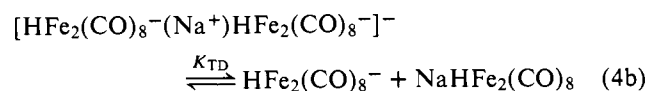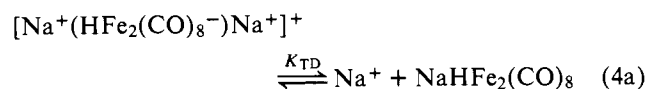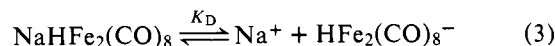**Figure 2.** Molar conductance, Λ, vs. $NaHFe_2(CO)_8$ concentration (open circles) or $(Na^+\text{-}crown)$ $(HFe_2(CO)_8^-)$ concentration (open squares) in THF.

$Fe_2(CO)_9$ is obtained which contains an iron–iron bond[26] of 2.523 (1) Å. The hydride in $NaHFe_2(CO)_8$ exhibits a ^1H NMR singlet at +8.47 ppm (upfield from Me_4Si) at 33 °C. The chemical shift of the hydride resonance is a function of temperature. It varies in an approximately linear fashion with temperature, shifting to 6.12 ppm (upfield from Me_4Si) at −66 °C. The proton-decoupled ^{13}C NMR of $NaHFe_2(CO)_8$ in THF shows a singlet at 223.8 ppm (downfield from Me_4Si) at approximately 25 °C. Even at −70 °C in THF, $NaHFe_2(CO)_8$ exhibits only a single ^{13}C CO resonance. Since bridging carbonyl bands are observed in the IR of $NaHFe_2(CO)_8$ in THF (vide infra), these ^{13}C NMR results require that bridging-to-terminal carbonyl exchange be rapid even at −70 °C. Without proton decoupling, the CO ^{13}C NMR resonance (226.8 ppm downfield from Me_4Si at −70 °C) is split by the hydride into a doublet, $J_{^{13}C-H}$ = 5.5 Hz. This rules out rapid intermolecular CO exchange at −70 °C.

Infrared bands for $NaHFe_2(CO)_8$ in THF were observed at 1987 (s), 1940 (s), 1880 (s), 1802 (sh), 1770 (m), and 1730 cm^{-1} (w). The 1770- and 1730-cm^{-1} absorptions are in a range typical of bridging carbonyls. The 1730-cm^{-1} peak arises from ion-pairing effects (vide infra).

Ion Pairing Studies. The molar conductance, Λ, vs. $[NaHFe_2(CO)_8]$ curve shows a minimum (Figure 2), characteristic[27] of systems that form triple ions (e.g., $[Na^+(HFe_2(CO)_8^-)\text{-}Na^+]^+$ and $[HFe_2(CO)_8^-(Na^+)HFe_2(CO)_8^-]^-$) and higher ion–ion aggregates as well as ion pairs and dissociated ions. We have observed similar behavior for $NaHFe(CO)_4$[28] and $NaRFe(CO)_4$[21b,29] in THF while others have observed this behavior for $NaCo(CO)_4$[30] and $(Mn(CO)_5^-)$[31] salts in THF. This Λ vs. concentration conductance behavior can be analyzed[27] in terms of the following two equilibria for ion-pair dissociation, K_D (eq 3), and triple-ion dissociation, K_{TD} (eq 4a and 4b).

$$NaHFe_2(CO)_8 \xrightleftharpoons{K_D} Na^+ + HFe_2(CO)_8^- \quad (3)$$

$$[Na^+(HFe_2(CO)_8^-)Na^+]^+$$
$$\xrightleftharpoons{K_{TD}} Na^+ + NaHFe_2(CO)_8 \quad (4a)$$

$$[HFe_2(CO)_8^-(Na^+)HFe_2(CO)_8^-]^-$$
$$\xrightleftharpoons{K_{TD}} HFe_2(CO)_8^- + NaHFe_2(CO)_8 \quad (4b)$$

Analysis of the Λ vs. $[NaHFe_2(CO)_8]$ data using eq 3 and 4 gives order of magnitude K_D and K_{TD} values for NaH-
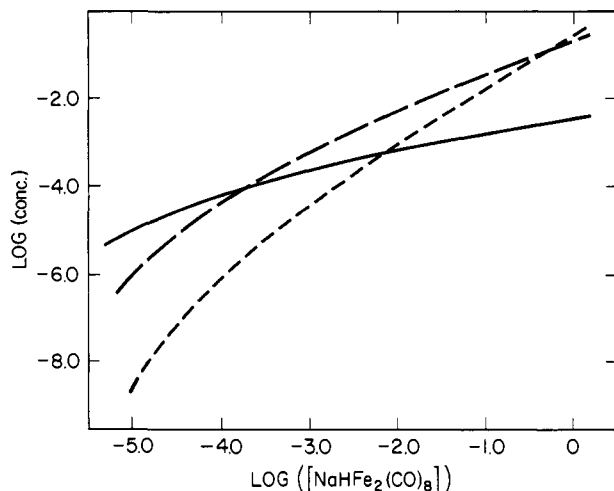
Figure 3. Calculated concentrations of tight-ion pairs (long dashes), triple ions (short dashes), and dissociated ions (solid line) as a function of the initial $NaHFe_2(CO)_8$ concentration in THF using eq 3 and 4 and $K_D = 7 \times 10^{-5}$ M; $K_{TD} = 3 \times 10^{-3}$ M.
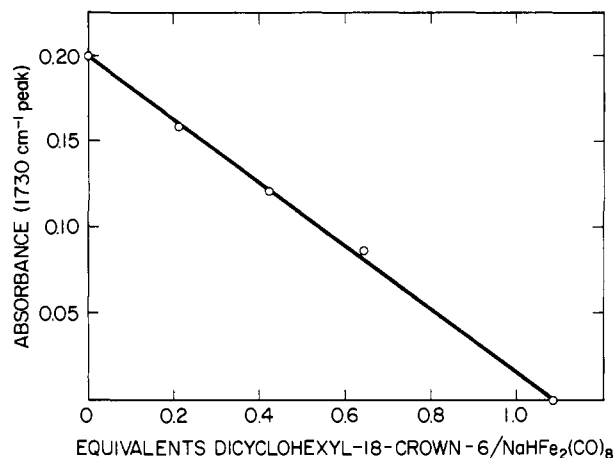

Figure 4. Crown ether titration of Na^+ from the bridging carbonyl (1730 cm^{-1}) of $HFe_2(CO)_8^-$ in THF.

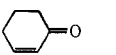Figure 5. Variation of the hydride chemical shift (parts per million relative to Me_4Si) upon complexation of Na^+ from $NaHFe_2(CO)_8$ with crown ether in THF.

$Fe_2(CO)_8$ in THF of[32] $K_D = 7 \times 10^{-5}$ M and $K_{TD} = 3 \times 10^{-3}$ M. The addition of 1 equiv of dicyclohexyl-18-crown-6/ $NaHFe_2(CO)_8$ increases the total conductance, but only by $\leq 37\%$ in the $NaHFe_2(CO)_8$ concentration range of $10^{-1}-10^{-3}$ M. Analysis of the Λ vs. $[(Na^+-crown)-(HFe_2(CO)_8^-)]$ curve yields order of magnitude K_{TD}' and K_D' values for $[(Na^+-crown)(HFe_2(CO)_8^-)]$ in THF of $K_D' = 2 \times 10^{-4}$ M and $K_{TD}' = 4 \times 10^{-3}$ M. Further support for the validity of these K_D and K_{TD} values is gained by the following observation. The metal carbonyl monoanions[29a] $NaRFe(CO)_4$ and[31] $M^+(Mn(CO)_5^-)$ ($M^+ = Li^+$, Na^+, Na^+-15-crown-5, and $Na^+-5HMPA$) all show K_D and K_{TD} values in the range $10^{-5}-10^{-4}$ and $10^{-3}-10^{-2}$, respectively, in THF. Using eq 3 and 4 and the K_D and K_{TD} values for $NaHFe_2(CO)_8$ in THF, the concentrations of triple ions, ion pairs and dissociated ions were calculated for the simultaneous equilibria presented in eq 3 and 4 as a function of the initial $[NaHFe_2(CO)_8]$. The results, Figure 3, show that below $\sim 10^{-4}$ M $[NaHFe_2(CO)_8]$, dissociated ions predominate while above 10^{-1} M ion pairs and triple ions predominate.

The Na^+ cation was found to be ion paired with one of the bridging carbonyls in $HFe_2(CO)_8^-$, giving rise to the 1730-cm^{-1} peak in the IR. Figure 4 shows that titration of a solution of $NaHFe_2(CO)_8$ with dicyclohexyl-18-crown-6 crown ether leads to a linear decrease in the absorbance of the 1730-cm^{-1} IR band with zero absorbance (within experimental error) at 1 equiv crown ether/$NaHFe_2(CO)_8$. The 1770-cm^{-1} band, which increased in absorbance concurrently with this decrease, has been tentatively assigned to bridging carbonyl(s) that are not ion paired to Na^+. Replacement of the Na^+ counterion by Li^+ shifts the 1730-cm^{-1} band to 1680 cm^{-1}. In the $[(Ph_3P)_2N]^+$ salt, the 1730-cm^{-1} band is absent, and has presumably been replaced by a higher frequency band which is buried under the other carbonyl bands. It is well known that Lewis acids prefer the better π-acid bridging vs. terminal carbonyls.[33]

Figure 5 shows that successive additions of dicyclohexyl-18-crown-6 shift the hydride ^1H NMR singlet of $NaHFe_2(CO)_8$ upfield in linear fashion, with a sharp break point at 1 equiv of crown ether/$NaHFe_2(CO)_8$.

Consistent with other studies,[29,31] the IR and conductivity ion pairing studies indicate that crown ether converts a mixture of tight and solvent-separated ion pairs into solvent-separated $(Na^+:S:HFe_2(CO)_8^-)$ without dramatically increasing the amount of dissociated species, $HFe_2(CO)_8^- + Na^+$. These
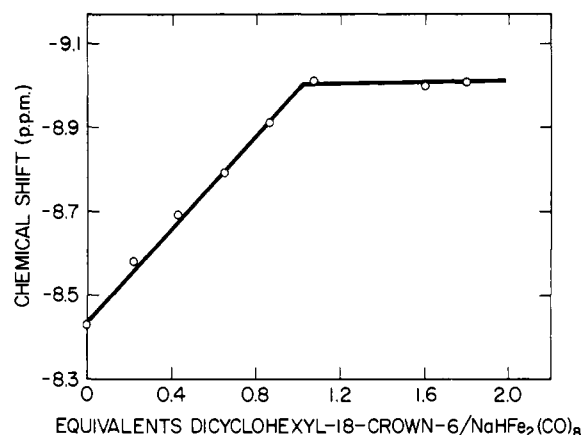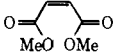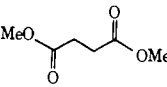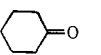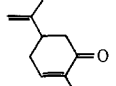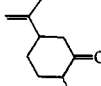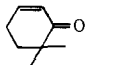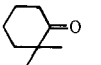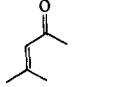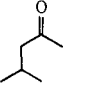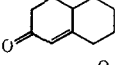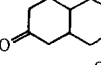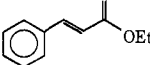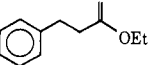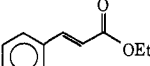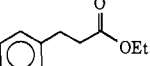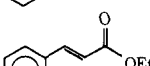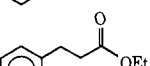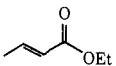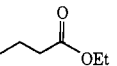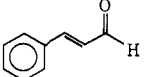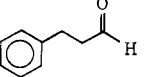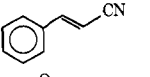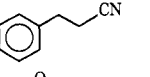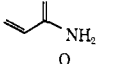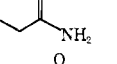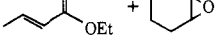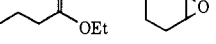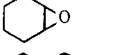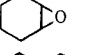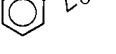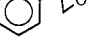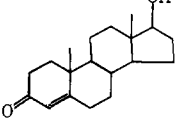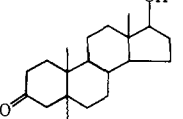
results emphasize the well-known need in ion-pairing studies to use a variety of physical techniques.[34] For example, although IR spectroscopy "sees" solvent-separated ion pairs as identical with dissociated ions,[34b] conductivity "sees" them as identical with tight ion pairs.

Synthetic Reductions Using $NaHFe_2(CO)_8$. Solutions of $NaHFe_2(CO)_8$ and HOAc in THF reduce the olefinic bond in α,β-unsaturated carbonyl compounds in high yield (Table I). The double bonds in unsaturated esters, ketones, aldehydes, nitriles, amides, and lactones were all reduced without concurrent carbonyl reductions. Epoxides are tolerated by the reagent alone (entries 16 and 17) or by the reagent actively reducing ethyl crotonate (15), demonstrating the mild conditions of these reductions. Carvone is reduced without isomerization or concurrent reduction of the isopropenyl group (3). $\Delta^{1,9}$-2-Octalone is reduced to 2-decalone with a cis:trans ratio of 4:1 (6). Testosterone is reduced with a cis:trans ratio of 10:1, although this yield and that of other bulky substrates was poor (18). Except for exceptionally active substrates like dimethyl maleate and mesityl oxide (1 and 5, respectively), 2 or more equiv of $NaHFe_2(CO)_8$ is required to reduce 1 equiv of substrate. Compared to acetic acid, the weak, insoluble acid, NH_4Cl, was found to increase yields, while the stronger acid Cl_3CCO_2H was found to decrease yields (7, 8, and 9, respectively). The initially puzzling $NaHFe_2(CO)_8$/substrate stoichiometry and the role of acid are now understood in detail and will be discussed in the mechanisms section.

In an effort to improve yields, it was found that faster, more

Table I. Reductions in THF

Entry	Substrate	Product	Yield[a]	Mol substrate: NaHFe$_2$(CO)$_8$:HOAc	Time, h
1			100	1/1/1	0.01
2			100	1/1.3/2.7	0.1
3			76 (35)[b]	1/5/5	20
4			97 (85)	1/2.5/2.5	1
5			87	1/1.2/1.2	0.25
6			45[c]	1/2/2	2
7			55	1/2/2	20
8			92[d]	1/2.2/2.2	20
9			5[e]	1/2/2	20
10			92	1/2.1/2.1	3
11			90 (76)	1/2.1/2.1	0.5
12			90	1/2/2	0.5
13			96	1/2/2	3
14			(50)	1/2/2	8
15			96 + 100	1/2.2/2.2	3
16			95	1/2/2	70
17			70	1/2/2	70
18			<10[f]	1/1.15/1.15	
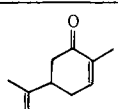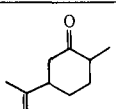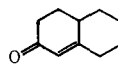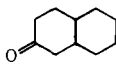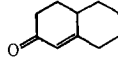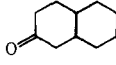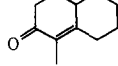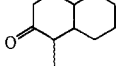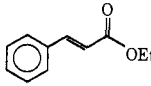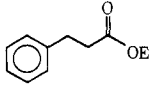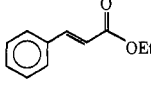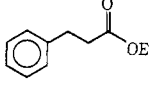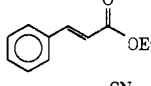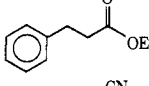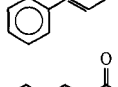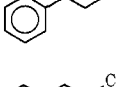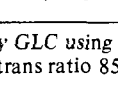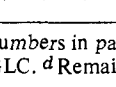
[a] Determined by VPC using internal standards. Numbers in parentheses correspond to isolated yields. [b] Cis 1,4:trans 1,4 ratio of 1:3.3 determined by ^{1}H NMR. [c] Cis to trans ratio 80:20 determined by GLC. [d] NH$_4$Cl used with Na$_2$Fe$_2$(CO)$_8$ instead of HOAc. [e] Cl$_3$CCO$_2$H used instead of HOAc. [f] Cis to trans ratio 10:1 determined by GLC.

effective reducing solutions were obtained by treating α,β-unsaturated carbonyl compounds with a heterogeneous slurry of Na$_2$Fe(CO)$_4$-1.5dioxane, Fe(CO)$_5$, and HOAc (Table II). Carbon monoxide evolution is not observed from Na$_2$-Fe(CO)$_4$-1.5dioxane and Fe(CO)$_5$ in dioxane, which is not surprising owing to the decreased nucleophilicity of Na$_2$-Fe(CO)$_4$ in dioxane.[21b,35] The addition of Fe(CO)$_5$ does increase yields however (5, 6, 2, and 3). Under these conditions

in dioxane, ethyl cinnamate is reduced to 77% in 0.5 h (5), in contrast to 50% in 20 h in THF. $\Delta^{1,9}$-2-Octalone (2) can be reduced quantitatively with a higher cis:trans ratio (87:13) than that observed in THF (80:20). However, some selectivity is lost under these conditions, as demonstrated by the reduction of aldehydes (9). As in reductions with NaHFe$_2$(CO)$_8$ in THF, weak acids like NH$_4$Cl increase the yields (5 and 7).

Reaction Stoichiometry in THF. The synthetic studies

Table II. Reductions in 1,4-Dioxane

Entry	Substrate	Product	Yield[a]	Mole ratios substrate:Na₂Fe(CO)₄: Fe(CO)₅:HOAc	Time, h
1			87	1/6/6/12	10
2			99 (91)[b]	1/6/6/12	16
3			93[c]	1/6/0/12	22
4			40[d]	1/6/6/12	16
5			77	1/1/1/2	0.5
6			58	1/1/0/2	1.5
7			100[e]	1/1.15/0/3.1	24
8			85	1/2/2/4	2
9			46	1/1.15/1.15/2.3	3

[a] Determined by GLC using internal standards. Numbers in parentheses correspond to isolated yields. [b] Cis to trans ratio 87:13 determined by GLC. [c] Cis to trans ratio 85:15 determined by GLC. [d] Remaining 60% is starting material. [e] NH₄Cl was used instead of glacial acetic acid.

demonstrated that in these reductions NaHFe₂(CO)₈ is required in a molar ratio of NaHFe₂(CO)₈/α,β-unsaturated carbonyl compound greater than one. The following evidence, obtained from a combination of GLC, NMR, IR, and product isolation studies, supports the stoichiometry presented in eq 5 for reductions by NaHFe₂(CO)₈ with HOAc present in THF:

$$2NaHFe_2(CO)_8 + trans\text{-}CH_3CH{=}CHCO_2Et + HOAc$$

$$IV$$

$$\xrightarrow[25.0\ °C]{THF} CH_3CH_2CH_2CO_2Et$$

$$V$$

$$+ NaHFe_3(CO)_{11} + Fe(CO)_5 + (NaOAc) \quad (5)$$
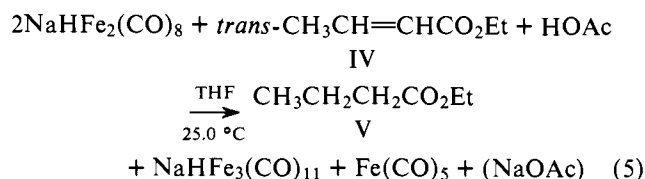
For reductions with *trans*-CH₃CH=CHCO₂Et in excess, the amount of reduced product, CH₃CH₂CH₂CO₂Et, was 50% by GLC (based on NaHFe₂(CO)₈). Furthermore, within 15% error,[36] the stoichiometry shown in eq 5 was demonstrated using 100-MHz ¹H NMR.

In the absence of HOAc, the mononuclear hydride NaHFe(CO)₄ was previously observed[21b,37] to add irreversibly and

$$NaDFe(CO)_4$$
$$+$$
$$CH_2{=}CHCO_2Et$$

$$\xrightarrow[2.5\ h]{25\ °C}\ THF$$

$$Na^+ \begin{bmatrix} CH_2(D)CHCO_2Et \\ | \\ Fe(CO)_4 \end{bmatrix} \xrightarrow{H^+} CH_2(D)CH_2CO_2Et$$

$$VI$$

isolated as PPN⁺ salt,
54% yield

$$(6)$$
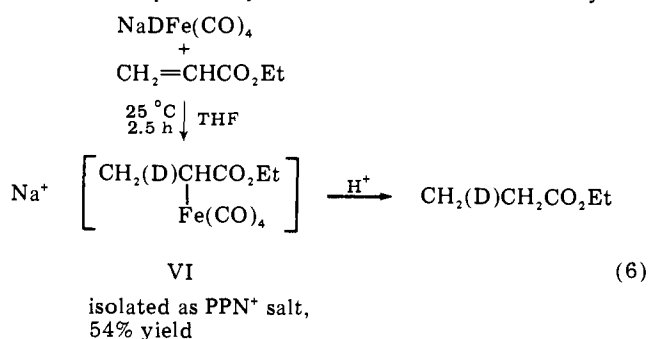
regiospecifically to ethyl acrylate giving an isolable alkyl iron product, VI, fully characterized by IR, NMR, and elemental analysis. This product rapidly gave ethyl propionate when treated with HOAc (eq 6). The intermediate alkyl iron product, VII, was also prepared independently[37a] by oxidative addition of CH₃CH(OTs)CO₂Et to Na₂Fe(CO)₄ and isolated as its PPN⁺ salt (eq 7).

$$Na_2Fe(CO)_4 + CH_3CH(OTS)CO_2Et$$

$$\xrightarrow[2.\ PPN^+Cl^-]{1.\ THF,\ -40\ to\ 25\ °C} [CH_3CH(Fe(CO)_4)CO_2Et]^- - PPN^+$$
$$VII\ (31\%\ yield) \quad (7)$$
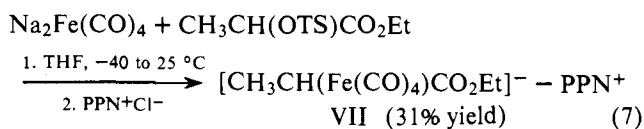
When NaHFe₂(CO)₈ reacts with *trans*-CH₃CH=CHCO₂Et in THF *without HOAc* (Table V, entry 6), the primary product is the monoiron alkyl, VIII. The product was identified by its ¹³C and 100-MHz ¹H spectra (Tables III and IV, respectively) which are identical with those of authentic VII prepared from NaHFe(CO)₄ and *trans*-CH₃CH=CHCO₂Et (eq 6). Addition of HOAc to the NMR sample tube converts all VII to CH₃CH₂CH₂CO₂Et in <1 min. The stoichiometry for the reaction of *trans*-CH₃CH=CHCO₂Et and NaHFe₂(CO)₈ in THF (no HOAc), established using a combination of GLC and NMR, is complex but appears to be that presented in eq 8.

$$3NaHFe_2(CO)_8 + 2\ trans\text{-}CH_3CH{=}CHCO_2Et$$

$$\xrightarrow[25.0\ °C]{THF} 2[Na^+[CH_3CH(Fe(CO)_4)CO_2Et]^-]$$

$$+ {\sim}1.0NaHFe_3(CO)_{11} + {\sim}1.0Fe(CO)_5 \quad (8)$$
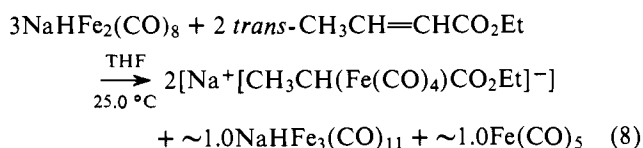
Some Na₂Fe₃(CO)₁₁ was also observed.[38] Again no Fe₃(CO)₁₂ was detectable by UV–visible spectroscopy.

Kinetic Studies in THF. Central to the kinetic results is the
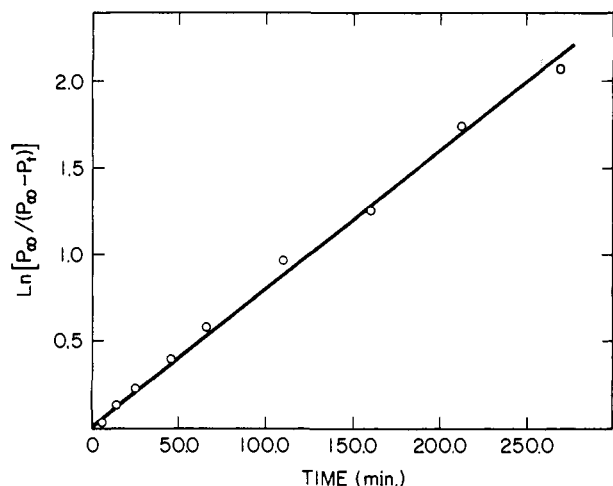
Figure 6. Representative GLC pseudo-first-order kinetic plot over 87% reaction for the reduction of *trans*-CH_3CH=$CHCO_2Et$ (in excess) by $NaHFe_2(CO)_8$ and HOAc (in excess). P_∞ and P_t are [ethyl butyrate] at completion and time = t, respectively.
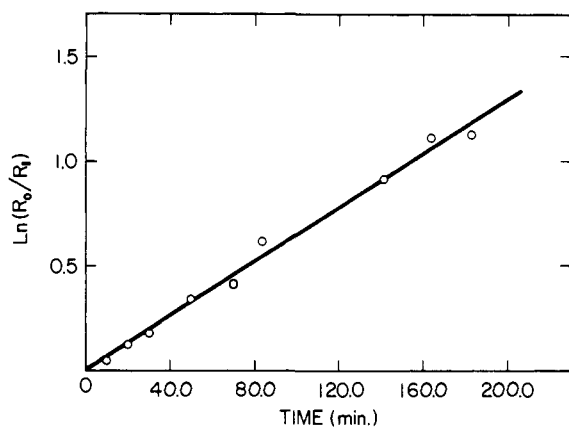
Figure 7. Representative GLC pseudo-first-order kinetic plot over 70% reaction for the reduction of *trans*-CH_3CH=$CHCO_2Et$ by $NaHFe_2(CO)_8$ (in excess) and HOAc (in excess, 0.088 M). R_0 and R_t = [*trans*-CH_3CH=$CHCO_2Et$] initially and at time = t, respectively.

method used to follow these reactions. *trans*-Ethyl crotonate was chosen as a model α,β-unsaturated carbonyl substrate since it is cleanly reduced in 100% yield (with excess $NaHFe_2(CO)_8$) in a convenient length of time, about 2–3 h. Since dimethyl maleate is reduced *at least* 50 times faster than *trans*-ethyl crotonate (Table VII, entries 1 and 6), the reduction of *trans*-ethyl crotonate and slower substrates could be stopped (quenched) by the addition of excess dimethyl maleate and HOAc. The reactants (e.g., *trans*-ethyl crotonate) and products (e.g., ethyl butyrate) could then be monitored simultaneously as a function of time by GLC (eq 9).

$$NaHFe_2(CO)_8 + trans\text{-}CH_3CH{=}CHCO_2Et$$

$$\xrightarrow[\substack{2.\ \text{quench (excess HOAc} + \\ \text{excess dimethyl maleate)}}]{1.\ \text{THF}} CH_3CH_2CH_2CO_2Et$$

$$+ CH_3CH{=}CHCO_2Et \quad \text{(analyzed by GLC)} \quad (9)$$
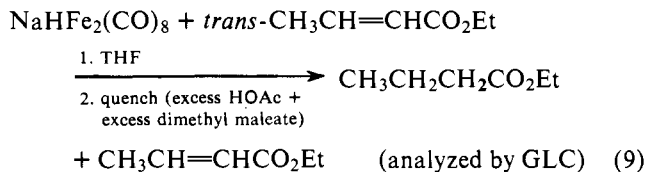
These kinetic results, performed with rigorous exclusion of oxygen and water using homogeneous, centrifuged $NaHFe_2(CO)_8$ solutions (no NaOAc present), are presented in Table V. A representative kinetic plot for reactions pseudo-first-order (with *trans*-ethyl crotonate and HOAc in excess) is presented in Figure 6, while a representative plot for reactions with $NaHFe_2(CO)_8$ in excess and 0.088 M HOAc is

Table III. ^{1}H NMR Data of $Na^+[CH_3CH_2CH(Fe(CO)_4)CO_2Et]^-$ Formed Either from $NaHFe_2(CO)_8$ and Ethyl Crotonate or of That Formed from $NaHFe(CO)_4$ and *trans*-Ethyl Crotonate

Chemical shift[a]	Assignment[b]
0.80 (t, J = 6.8 Hz)	H-6
1.18 (t, J = 7.3 ± 0.7 Hz)[c]	H-1
1.96–2.38 (multiplet, major peaks at 2.24, 2.28, 2.35, 2.38)	H-2, H-3[d]
3.96 (q, J = 7.0 Hz)	H-5

[a] In parts per million, benzene (7.266 ppm) used as a standard (downfield = positive). [b] $[C^1H_3C^2H_2C^3H(Fe(CO)_4)C^4O_2\text{-}C^5H_2C^6H_3]^-$. [c] Overlap with residual ethyl crotonate peaks prevents accurate measure of the coupling constant. [d] Assignment of these peaks was prevented owing to the proximity of residual THF-d_8 resonances.

Table IV. ^{13}C NMR Data of $Na^+[CH_3CH_2CH(Fe(CO)_4)CO_2Et]^-$ Formed Either from $NaHFe_2(CO)_8$ and Ethyl Crotonate or of That Formed from $NaHFe(CO)_4$ and Ethyl Crotonate

Chemical shift[a]	Rel intensity[b]	Assignment[c]
221.64	0.61	C-7
189.79	0.064	C-4
58.77	1.00	C-5
32.07	0.75	C-3
24.45	0.37	C-2
17.61	0.87	C-1
14.62	0.87	C-6

[a] In parts per million from internal tetramethylsilane (downfield = positive). [b] Relative intensities were run under identical conditions and are for comparison only. [c] $[C^1H_3C^2H_2C^3H(Fe(C^7O)_4)\text{-}C^4O_2C^5H_2C^6H_3]^-$.

shown in Figure 7. The validity of this GLC kinetic method was checked by monitoring the reduction reaction directly by ^{1}H NMR in THF-d_8. Kinetics by ^{1}H NMR (entries 2 and 6, Table V) gave the same rate constants within experimental error as the GLC kinetic method (5 and footnote d). The kinetic data clearly demonstrate that the reductions of *trans*-ethyl crotonate by $NaHFe_2(CO)_8$ are first order in *trans*-ethyl crotonate (Figure 8) and first order in $NaHFe_2(CO)_8$ both with HOAc in excess (Figure 9) and without HOAc present (Figure 10). It should be noted that owing to the 2:1 $NaHFe_2(CO)_8$ to *trans*-CH_3CH=$CHCO_2Et$ stoichiometry of reductions with HOAc present (eq 5), $-d[NaHFe_2(CO)_8]/dt$ = $2(-d[trans\text{-}CH_3CH{=}CHCO_2Et]/dt)$. For this reason the rate constants for reactions run pseudo-first-order with [*trans*-CH_3CH=$CHCO_2Et$] in excess must be divided by this statistical factor of 2 in order to be directly comparable to the rate constants run with $NaHFe_2(CO)_8$ in excess. Divisions by this statistical factor of 2 have already been performed wherever required. (See footnote a, Table V.) Although semilog plots were routinely linear over 3 half-lives for reactions with HOAc and *trans*-ethyl crotonate in excess (Figure 6), plots for reactions with $NaHFe_2(CO)_8$ in excess and without HOAc or with $\geq$0.088 M HOAc deviate from linearity.[39] Thus, initial rates have been used for reactions under those conditions which did not give linear semilog plots. The deviations caused by excess HOAc have been studied in some detail, and are due to an acid-dependent $NaHFe_2(CO)_8$ decomposition path. These results will be presented in the section entitled "Studies of $NaHFe_2(CO)_8$ Decomposition Mechanisms".

In spite of the initial problems caused by acid-dependent $NaHFe_2(CO)_8$ decomposition, the dependence of these reduction reactions upon [HOAc] has been clearly established. The results, measured with $NaHFe_2(CO)_8$ and HOAc in ex-

Table V. Kinetic Data for *trans*-CH₃CH=CHCO₂Et Reductions Using NaHFe₂(CO)₈ in THF

Entry	[NaHFe₂(CO)₈], M	[CH₃CH=CHC-O₂Et], M	[HOAc], M	Other exptl information	$k_2(\text{obsd})^a \times 10^3$, $M^{-1} s^{-1}$
		Reactions Run Pseudo-First-Order with NaHFe₂(CO)₈ in Excess			
1	0.20, 0.10,[b] and 0.05	0.01	0.088		1.0 ± 0.1^c
2	0.20	0.20	0.12	Reaction monitored directly by ¹H NMR in THF-d_8	$\sim 0.9^d$
3	0.10	0.01	0.088 DOAc	NaDFe₂(CO)₈ and DOAc used	2.4 (k_D/k_H = 2.4 ± 0.3)[e]
4	0.10	0.01	0.088	0.10 M NaHFe(CO)₄	3.3
5	0.20, 0.10,[f] and 0.05	0.01	None		0.70 ± 0.05^c
6	0.20	0.20	None	Reaction monitored directly by ¹H NMR in THF-d_8	0.74^g
7	0.10	0.01	None	NaDFe₂(CO)₈ used	2.4 (k_D/k_H = 3.5 ± 0.5)[e]
8	0.10	0.01	None	0.10 M NaHFe(CO)₄ added	~ 9
		Reactions Run Pseudo-First-Order with CH₃CH=CHCO₂Et in Excess			
9	0.01	0.38, 0.20,[h] and 0.10	0.088		0.65 ± 0.01^c
10	0.01	0.20	0.088	0.10 M Fe(CO)₅ added	0.79
11	0.01	0.20	0.088	Run pseudo-first-order, P_{CO} = (1 atm)	0.28^i
12	0.01	0.10	None		0.45^j

[a] All data at 25.0 ± 0.1 °C. For reactions with [HOAc] and [NaHFe₂(CO)₈] or [CH₃CH=CHCO₂Et] in excess, $k_2(\text{obsd})$ = $k_1/[\text{NaHFe}_2(\text{CO})_8]$ or $k_2(\text{obsd})$ = $k_1/[\text{CH}_3\text{CH=CHCO}_2\text{Et}]$, respectively. Also, $k_2(\text{obsd})$ = $k_{2R} + k_{3R}[\text{HOAc}]$ (see Figures 11 and 12). $k_2(\text{obsd})$ is the average of the least-squares rate constants for k_2(reactants) (e.g., monitoring the disappearance of ethyl crotonate) and k_2(products) (e.g., monitoring the formation of ethyl butyrate) for reactions with [NaHFe₂(CO)₈] and [HOAc] in excess. For reactions with [HOAc] and [CH₃CH=CHCO₂Et] in excess, $k_2(\text{obsd})$ = k_2(products)/2, since the stoichiometry is 2NaHFe₂(CO)₈/1CH₃CH=CHCO₂Et, and thus $-d[\text{HFe}_2(\text{CO})_8]/dt = 2(-d[\text{CH}_3\text{CH=CH}_2\text{CO}_2\text{Et}]/dt)$. For reactions with [NaHFe₂(CO)₈] only in excess (no HOAc), initial rates were used to calculate $k_2(\text{obsd})$. [b] See Figure 9. [c] These error limits indicate the reproducibility of three experiments (1 standard deviation). [d] $k_2(\text{obsd})$ (25 ± 2 °C) was calculated from the average initial rates of CH₃CH=CHCO₂Et disappearance and [CH₃CH₂CH₂CO₂Et] appearance. The GLC kinetic method gives $k_2(\text{obsd})$ = 1.2×10^{-3} M⁻¹ s⁻¹ at 0.12 M HOAc (see Figure 11). [e] Standard deviation assuming 10% precision in each rate constant. [f] See Figure 10. [g] The disappearance of [CH₃CH=CHCO₂Et] was monitored and the initial reaction rate and initial concentrations were used to calculate $k_2(\text{obsd})$. [h] See Figure 8. [i] There is a concurrent reaction occurring, NaHFe₂(CO)₈ + CO → NaHFe(CO)₄ + Fe(CO)₅. For conditions with constant [CH₃CH=CHCO₂Et] and [CO], the first-order rate constant for the appearance of CH₃CH₂CH₂CO₂Et has the following form: $k_1(\text{obsd})$ = k_2(CO reaction)$[P_{CO}]$ + $2k_2(\text{obsd})[\text{CH}_3\text{CH=CHCO}_2\text{Et}]$, with $k_1(\text{obsd})$ = 2.78 $\times 10^{-4}$ s⁻¹. Since the yield of CH₃CH₂CH₂CO₂Et was 39% its usual value, $(100 - 39)/39 = 1.56 = k_2(\text{CO reaction})[P_{CO}]/(2k_2(\text{obsd}) \cdot [\text{CH}_3\text{CH=CHCO}_2\text{Et}])$. These values give, at 1 atm of CO, k_2(CO reaction) $[P_{CO}]$ = 1.7×10^{-4} s⁻¹ and $k_2(\text{obsd})$ = 2.8×10^{-4} M⁻¹ s⁻¹. [j] Since the stoichiometry without HOAc present is 3NaHFe₂(CO)₈/2CH₃CH=CHCO₂Et, $k_2(\text{obsd})$ = k_2(products)/(3/2).
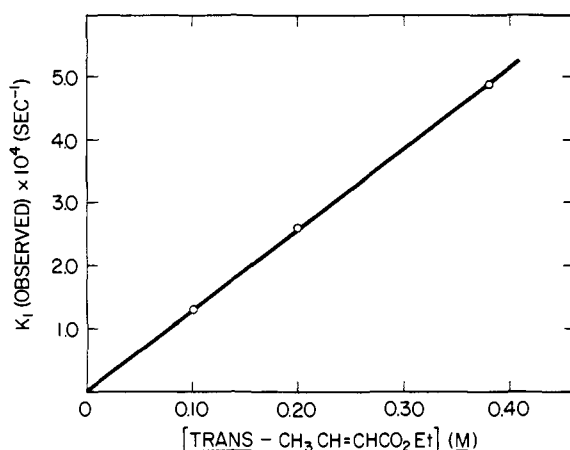
Figure 8. Linear dependence of the pseudo-first-order rate constant upon the concentration of (excess) *trans*-CH₃CH=CHCO₂Et for its reduction to CH₃CH₂CH₂CO₂Et. (The k_1(obsd) values have not been divided by the statistical factor of 2.)
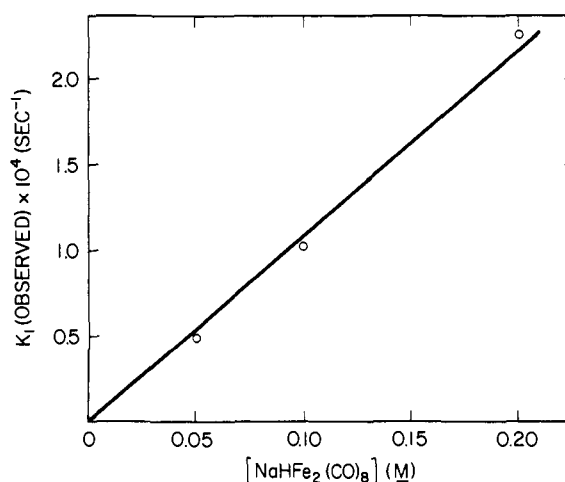
Figure 9. Linear dependence of the pseudo-first-order rate constant upon the concentration of (excess) NaHFe₂(CO)₈ with HOAc (0.088 M) present for *trans*-CH₃CH=CHCO₂Et reduction.

cess, indicate that these reductions follow an acid-dependent as well as acid-independent path, $k_2(\text{obsd})$ = $k_{2R} + k_{3R}$· [HOAc] (Figure 11). Least-squares analysis of the data gives (error bars represent one standard deviation) k_{2R} = 6.2 ± 0.5 $\times 10^{-4}$ M⁻¹ s⁻¹; k_{3R} = 5.3 ± 0.3 × 10⁻³ M⁻² s⁻¹. As a check upon these data, the [HOAc] dependence of these reductions

was established using *trans*-CH₃CH=CHCO₂Et and HOAc in excess (Figure 12). Again k_2 (obsd) = $k_{2R} + k_{3R}$[HOAc], with slope = 9.5 ± 0.4 × 10⁻³ M⁻² s⁻¹, intercept = 6.6 ± 0.8 × 10⁻⁴ M⁻¹ s⁻¹. After dividing by the appropriate statistical factor introduced by the reaction stoichiometry (slope/2 and intercept/2), k_{3R} = 4.7 ± 0.2 × 10⁻³ M⁻² s⁻¹ and k_{2R} = 4.4
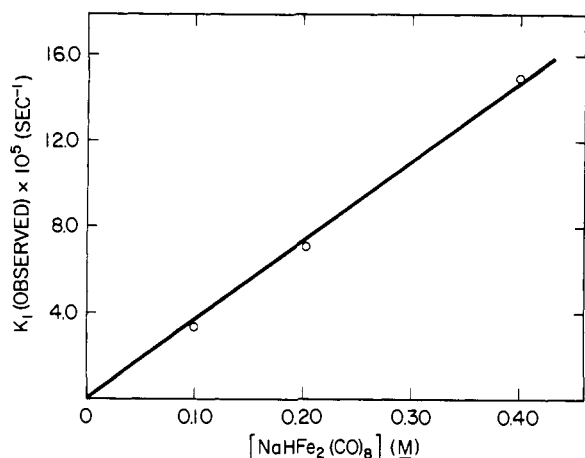
Figure 10. Linear dependence of the initial pseudo-first-order rate constant upon the concentration of (excess) $NaHFe_2(CO)_8$ for *trans*-CH_3CH=$CHCO_2Et$ reduction.
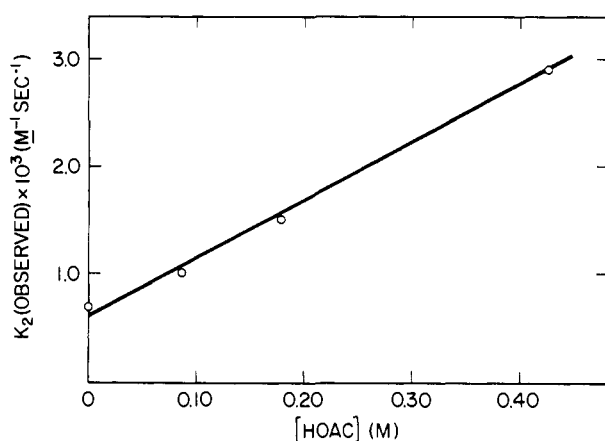
Figure 11. Linear dependence of the initial second-order rate constant upon the concentration of (excess) HOAc for *trans*-CH_3CH=$CHCO_2Et$ reduction with $NaHFe_2(CO)_8$ in excess.

$\pm$ 0.5 $\times$ 10^{-4} M^{-1} s^{-1}. The agreement between the two k_3 values is reasonably good (k_{3R} = 5.3 $\pm$ 0.3 $\times$ 10^{-3} and 4.7 $\pm$ 0.2 $\times$ 10^{-3} M^{-2} s^{-1}). The k_{2R} values (k_{2R} = 6.2 $\pm$ 0.5 and 3.3 $\pm$ 0.4 $\times$ 10^{-4} M^{-1} s^{-1}) differ by more than experimental error. However, some decrease in k_{2R} at lower $[NaHFe_2(CO)_8]$ is expected owing to ion-pairing effects (vide infra).

In order to determine whether reversible iron–iron bond cleavage in $NaHFe_2(CO)_8$ to give $NaHFe(CO)_3$ + $Fe(CO)_5$ or $NaHFe(CO)_4$ + $Fe(CO)_4$ is occurring in these reduction reactions, possible inhibition by added $Fe(CO)_5$ or $NaHFe(CO)_4$ was examined. Added $Fe(CO)_5$ (0.5 equiv $Fe(CO)_5$/$NaHFe_2(CO)_8$) has no effect on k_2 (obsd) within experimental error (entry 10, Table V). Surprisingly, added $NaHFe(CO)_4$ *increases* the rate of $NaHFe_2(CO)_8$ addition to *trans*-ethyl crotonate (no HOAc present) (8). In the presence of HOAc, the $NaHFe(CO)_4$-induced rate increase is less (4).

The rate of *trans*-ethyl crotonate reduction was measured under 1 atm of CO pressure to see if the equilibrium $NaHFe_2(CO)_8$ ⇌ $NaHFe_2(CO)_7$ + CO is involved in these reduction reactions. Although the kinetics are complicated owing to a CO-induced decomposition of $NaHFe_2(CO)_8$, we have obtained a quantitative measure of the CO inhibition of these reduction reactions (see footnote *i*, Table V). We found that 1 atm of CO inhibited the reductions about 2.3-fold (entry 11, Table V), far less than that expected if reversible CO dissociation had been involved in these reduction reactions.

The deuterium isotope effect, the effect of ion pairing, and
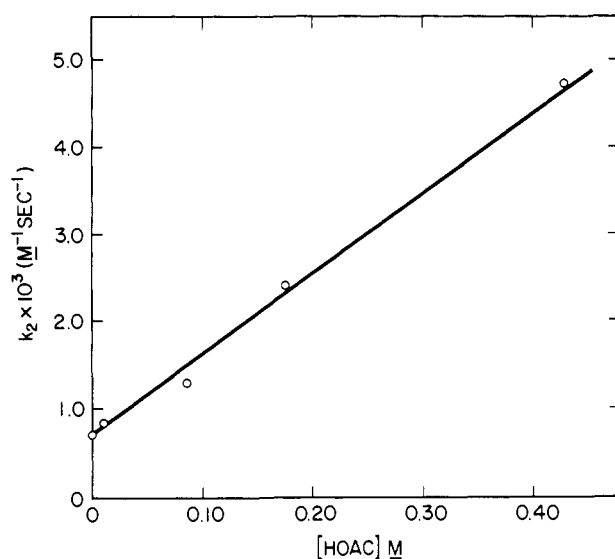
Figure 12. Linear dependence of the second-order rate constant upon the concentration of (excess) HOAc with *trans*-CH_3CH=$CHCO_2Et$ (in excess).

Table VI. Ion-Pairing Effects for[a]
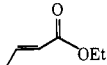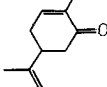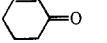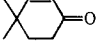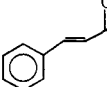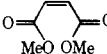
$$M^+[HFe_2(CO)_8]^- + trans\text{-}CH_3CH\text{=}CHCO_2Et \xrightarrow[25.0\ °C]{THF}$$

Entry[a]	HOAc, M	Cation (M^+)	Other exptl information	k_2(obsd) $\times$ 10^3, M^{-1} s^{-1} [b]
1	None	Na$^+$	0.20 M NaBPh$_4$ added[c]	0.76
2	None	Li$^+$		0.85
3	None	Na$^+$	4.7% (v/v) NMP/THF added[d]	0.13
4	None	Na$^+$	1 equiv (0.1 M)[e] dicyclo-hexyl-18-crown-6 added	0.22
5	0.088	Na$^+$	0.20 M NaBPh$_4$ added[c]	1.0
6	0.088	Li$^+$		1.0
7	0.088	Na$^+$	4.7% (v/v) NMP/THF[d] added	0.38
8	0.088	[(Ph$_3$P)$_2$N]$^+$		0.36

[a] All reactions at $[M^+(HFe_2(CO)_8)^-]$ = 0.10 M, $[CH_3CH$=$CHCO_2Et]$ = 0.01 M. [b] k_2(obsd) = k_{2R} + $k_{3R}[HOAc]$. Initial rates were used to calculate k_2(obsd). [c] K(dissociation) for NaBPh$_4$ in THF is 8.5 $\times$ 10^{-5} M: J. Smid and M. Szwarc, *J. Phys. Chem.*, **69**, 608 (1965). Thus a 0.20 M NaBPh$_4$/THF solution gives 4.1 $\times$ 10^{-3} M Na$^+$ ions. [d] 4.7% NMP (*N*-methylpyrrolidinone) under these conditions is 5.2 equiv NMP/Na$^+$. [e] A mixture of A and B isomers was used.

relative substrate reactivities have also been examined for reductions using $NaHFe_2(CO)_8$. An unusual, large inverse k_D/k_H deuterium isotope effect is observed. With no DOAc present and using $NaDFe_2(CO)_8$, an inverse deuterium isotope effect of k_D/k_H = 3.5 was observed (7). The deuterium isotope effect is acid dependent. In the presence of 0.088 M DOAc, k_D/k_H = 2.4 (3).

In previous studies, we have shown that the chemistry of $Na_2Fe(CO)_4$[21b,35] and $NaRFe(CO)_4$[21b,29] is dominated by ion-pairing phenomena. Since conductance studies showed that $NaHFe_2(CO)_8$ can exist in THF as a mixture of dissociated ions, ion pairs, triple ions (eq 3 and 4), and higher aggregates, the effect of ion pairing in these reduction reactions was examined. The results presented in Table VI show that, as expected, ion pairing is important in reductions by (HFe_2-

Table VII. Substrate Relative Reduction Rates

Entry[a]	Substrate	k_2 (obsd),[b] M^{-1} s^{-1}	Rel rates	$E_{1/2}$ redn[c] potential, V vs. SCE
1	(structure: CH₂=CH–C(=O)–OEt)	1.0×10^{-3}	1.0	−2.3
2	(structure: cyclohexenone with methyl and isopropenyl substituents)	$\sim2.0 \times 10^{-4}$	~0.2	−2.2
3	(structure: cyclohexenone)	$>5.0 \times 10^{-2}$	>50	−2.07
4	(structure: 4,4-dimethylcyclohexenone)	$\sim4.6 \times 10^{-2}$	~46[d]	−2.0
5	(structure: PhCH=CH–C(=O)–OEt, cinnamate)	$\sim3.0 \times 10^{-4}$	~0.3[e]	−1.81
6	(structure: O=C–C=C–C=O with MeO OMe)	$>5.0 \times 10^{-2}$	>50	

[a] All reactions were run at 0.10 M NaHFe₂(CO)₈, 0.01 M substrate, and 0.088 M HOAc at 25.0 °C in THF. [b] For entries 2 and 5, k_2 (obsd) was calculated from initial rates and initial concentrations. [c] $E_{1/2}$ reduction potentials in DMF; H. O, House, L. E. Huber, and M. J. Umen, *J. Am. Chem. Soc.*, 94, 8471 (1972). The values for entries 2 and 4 were calculated using House's empirical rules. [d] For NaDFe₂(CO)₈ and DOAc, k(obsd) $\approx 8.2 \times 10^{-2}$ M^{-1} s^{-1}; $k_D/k_H \approx$ 1.8. [e] For NaDFe₂(CO)₈ and DOAc, k(obsd) $\approx 7.5 \times 10^{-4}$ M^{-1} s^{-1}; $k_D/k_H \approx 2.5$.

(CO)₈)⁻. For example, added cation complexing crown ether (1 equiv of dicyclohexyl-18-crown-6/NaHFe₂(CO)₈) slows the reaction 3.2-fold (entry 4, Table VI). However, these ion-pairing rate effects are much less than those of 10^3–10^4 previously observed for NaRFe(CO)₄ and Na₂Fe(CO)₄ reactions, respectively. The rates of reductions by $M^+[HFe_2(CO)_8]^-$ are also dependent upon the cation, M^+. The rates decrease in THF for Li⁺ > Na⁺ > PPN⁺.

Relative α,β-unsaturated carbonyl substrate reactivities have also been determined (Table VII). These results show that substitution α or γ to the carbonyl slows these reactions (entries 2, 3, and 4, Table VII), and cis isomers usually react rapidly (3). In general, our synthetic studies of reductions by NaHFe₂(CO)₈ show that these reactions are inhibited by sterically bulky substrates. (See, for example, entry 18, Table I.)

Entries 1–5, Table VII, show that there is no obvious correlation of k_2 (obsd) with the $E_{1/2}$ reduction potentials. In the absence of steric effects and if electron transfer were the rate-determining step, one would expect such a correlation.

Deuterium Isotope Labeling and Stereochemical Studies. Since the addition of the monoiron deuteride, DFe(CO)₄⁻, to CH₂=CHCO₂Et is regiospecific and irreversible (eq 6), it was of interest to see if reductions using binuclear NaHFe₂(CO)₈ also showed this chemistry. The observation of an inverse isotope effect for NaHFe₂(CO)₈ reductions suggests that NaHFe₂(CO)₈ additions were, however, reversible, since this inverse isotope effect can be quantitatively explained as an equilibrium isotope effect (see the Discussion section).

Additional evidence for reversible addition of DFe₂(CO)₈⁻ is presented in Table VIII, entry 1. Thus, GLC–mass spectral analysis after 60% completion of the reaction of 0.2 M NaDFe₂(CO)₈, 0.09 M DOAc, and 0.05 M PhCH=CHCO₂Et in THF shows that the reduced product contains up to three *but not four* deuterium atoms. The observation of d_3 product requires reversible addition of deuterium to the double bond. Furthermore, this reversibility coupled with the lack of d_4-containing product requires that this deuterium addition be regiospecific. Examination of the (PhCH₂)⁺ mass

Scheme I. Proposed Mechanism to Account for the Low d_1/d_0 Ratio Observed for the Reduction of PhCH=CHCO₂Et by NaDFe₂(CO)₈ and DOAc
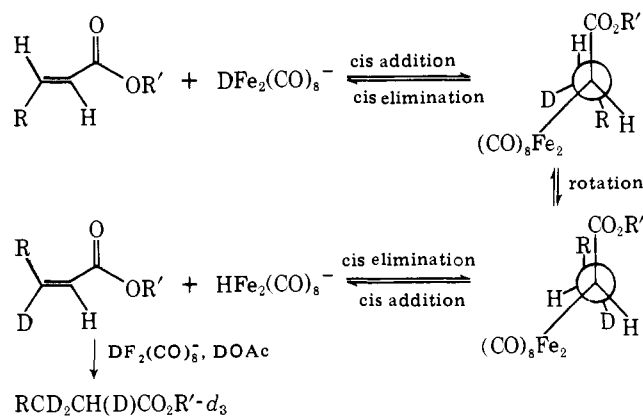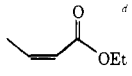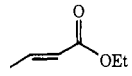
spectral fragment shows significant amounts of a d_2-containing fragment (PhCD₂)⁺, suggesting that the deuterium from NaDFe₂(CO)₈ adds regiospecifically β to the carbonyl in PhCH=CHCO₂Et. Analysis of the unreacted PhCH=CHCO₂Et shows that it contains up to ~25% d_1 but no d_2, offering further support for the reversibility and regiospecificity of this reaction. Reversibility in the reaction of 0.2 M *trans*-CH₃CH=CHCOEt and 0.2 M NaDFe₂(CO)₈ in THF-d_8 was established by 100-MHz ¹H NMR. During this reaction at 25 °C, the doublet due to the α proton in *trans*-CH₃CH=CHCO₂Et (5.79 ppm, relative to Me₄Si) is replaced by a broad singlet due to the formation of *trans*-CH₃CD=CHCO₂Et.

This reversibility and regiospecificity is not unprecedented. The addition of HCo(CN)₅³⁻ to α,β-unsaturated carbonyl compounds is reversible and regio*selective*[40] while H₂Os₃(CO)₁₀ additions to α,β-unsaturated carbonyl compounds are also reversible and apparently regiospecific.[7a]

In order to test the stereospecificity of these reductions, the reduction of 0.05 M 4,4-dimethylcyclohexenone by 0.2 M NaDFe₂(CO)₈ and 0.1 M DOAc in THF was examined (entry 2, Table VIII). Analysis by GLC–MS of the reduced product shows that it contains up to two, but not three, deuteriums. This result, coupled with the knowledge that these DFe₂(CO)₈⁻ additions are reversible, *requires that these reductions are highly stereoselective and probably stereospecific.* (The reductions of 4,4-dimethylcyclohexenone also show an inverse isotope effect, $k_D/k_H \sim 1.8$ (Table VII, entry 4) which will be interpreted later, in detail, as evidence for this reversibility.) However, the overall stereochemistry of reduction, either net cis or trans addition of H₂, is not known. These results suggest that the formation of d_3-containing reduced product in acyclic α,β-unsaturated substrates, such as PhCH=CHCO₂Et, proceeds via trans ⇌ cis isomerization, as outlined in Scheme I.

Consistent with this scheme is the observation of significant amounts of PhCH=CHCO₂Et-d_0 and PhCHDCHDCO₂Et-d_2 in the reaction of NaDFe₂(CO)₈ and PhCH=CHCO₂Et. Naively, for a rapid reversible addition of DFe₂(CO)₈⁻, one would expect only PhCD=CHCO₂Et-d_1 and thus only PhCD₂CHDCO₂Et-d_3. However, the apparent stereospecificity of this addition (and thus of the elimination by microscopic reversibility) requires the formation of PhCD=CHCO₂Et-d_1 via *cis*-PhCD=CHCO₂Et, and thus the d_1/d_0 ratio reflects the low equilibrium ratio of cis/trans. Scheme I predicts that *cis*-RCH=CHCO₂R′ should be rapidly rearranged to *trans*-RCD=CHCO₂R′ by NaDFe₂(CO)₈. Unfortunately, an alternate mechanism for cis to trans isomerization exists so that the hypothesis cannot be tested. Entry

Table VIII. Isotopic Labeling Studies Using $NaDFe_2(CO)_8$ and CH_3CO_2D

Entry	Recovered reactant	Fragment	Mol wt	$d_0/d_1/d_2/d_3{}^a$	Product		Mol wt	$d_1/d_2/d_3/d_4{}^a$
1	PhCH=CHCO₂Et[b]			10.0/3.3/0.0 (10.0/1.0/0.0)	PhCH₂CH₂CO₂Et	(Parent)⁺·	178	5.5/10.0/1.2/0.0 (4.2/10.0/1.7/0.0)
		(Parent)⁺·	176			(PhCH₂CH₂CO)⁺	133	6.3/10.0/1.9/0.0 (6.6/10.0/1.1/0.0)
		(PhCH=CHCO₂)⁺	148	10.0/2.4/0.0 (10.0/1.5/0.0)		(PhCH₂)⁺	91	(d_0) 2.1/10.0/0.84/0.0 (2.5/10.0/0.56/0.0)
2				(Not determined)		(Parent)⁺·	126	(d_1) 2.8/10.0/0.0
3				(Not determined)		(Parent)⁺·	114	d_0/d_1 10.0/0.0

[a] Ratios were determined by GLC–mass spectrometry. Raw relative abundances were corrected for the amount of M + 1 peak observed in the GLC–mass spectrum of authentic materials. The largest peak has been normalized to 10.0. [b] Mass spectral data for the reaction of 0.1 M each of $NaDFe_2(CO)_8$ and PhCH=CHCO₂Et. After 86% reaction, the mixture was quenched with excess DOAc. The numbers in parentheses are for a repeat reaction of 0.2 M $NaDFe_2(CO)_8$, 0.09 M DOAc and 0.05 M PhCH=CHCO₂Et, which was stopped after 60% reaction. [c] For the reaction at 100% conversion of 0.2 M $NaDFe_2(CO)_8$, 0.1 M DOAc, and 0.5 M 4,4-dimethylcyclohexenone. [d] For the reaction of 0.2 M $NaDFe_2(CO)_8$, 0.08 M DOAc, and 0.04 M cis-CH₃CH=CHCO₂Et. After 1.2 min the reaction was quenched with dimethyl maleate and DOAc, and GLC analysis showed that the cis isomer had been converted to the equilibrium mixture of ~90% trans plus ~10% cis.
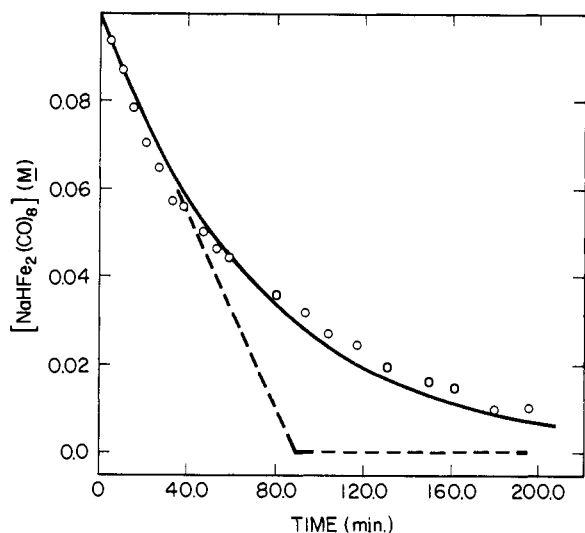
Figure 13. The concentration of $NaHFe_2(CO)_8$ vs. time for the reaction $NaHFe_2(CO)_8 + CO \rightarrow NaHFe(CO)_4 + Fe(CO)_5$ in the presence of 0.177 M HOAc under a constant CO pressure, $P_{CO} = 1$ atm. The reaction was monitored by volumetric CO uptake (open circles). The solid line is the calculated $[NaHFe_2(CO)_8]$ vs. time obtained by numerical integration (fourth order Runge-Kutta) of concurrent decomposition and CO substitution pathways. The dashed line represents the measured rate of CO (gas) → CO (solution) under these conditions.

3, Table VIII shows that, although cis-CH₃CH=CHCO₂Et is rearranged to ~90% trans-CH₃CH=CHCO₂Et (plus ~10% cis-CH₃CH=CHCO₂Et) ≥100 times faster (≤1.2 min) than the rate of its reduction, the resulting product contains no trans-CH₃CD=CHCO₂Et-d_1. The fact that a 0.1 M $NaHFe_2(CO)_8$ solution isomerized cis-hex-3-ene to trans-hex-3-ene within 20 min, although such unactivated olefins are not reduced, demonstrates this alternate cis to trans isomerization mechanism. Also, rearrangement to 1- or 2-hexenes was not observed. Since metal radicals in $NaHFe_2(CO)_8$ solutions have been identified by ESR (vide infra), this cis to trans isomerization may involve these radicals.

In addition to this rapid cis–trans isomerization, we have uncovered an additional side reaction catalyzed by NaHFe₂(CO)₈ solutions which is also quite possibly radical in nature. Analysis by GLC–MS at 60% completion (DOAc and

dimethyl maleate quench) of the reaction of 0.2 M $NaDFe_2(CO)_8$, 0.10 M DOAc, and 0.05 M trans-CH₃CH=CHCO₂Et shows that up to three deuteriums are incorporated into the unreduced trans-CH₃CH=CHCO₂Et while up to five deuteriums are incorporated into CH₃CH₂CH₂CO₂Et. Analysis of the m/e 71 $(CH_3CH_2CH_2CO)^+$ fragment shows that no deuterium was incorporated into the ethyl ester, but that the activated allylic methyl group must have incorporated deuterium.

Finally, attempts to determine whether reductions by $NaHFe_2(CO)_8$ and HOAc proceed with overall cis or trans addition by using dimethyl maleate (cis-CH₃O₂CH=CHCO₂CH₃) and dimethyl fumarate (trans-CH₃O₂CH=CHCO₂CH₃) have failed.[41]

Reaction of $NaHFe_2(CO)_8$ with CO, ^{13}CO, and PPh_3. As observed with many cluster compounds,[1b,1e] added CO cleaves the metal–metal bond in $NaHFe_2(CO)_8$. The products are shown in the equation

$$NaHFe_2(CO)_8 + CO \xrightarrow[\text{THF}]{k_{CO}} NaHFe(CO)_4 + Fe(CO)_5$$

(10)
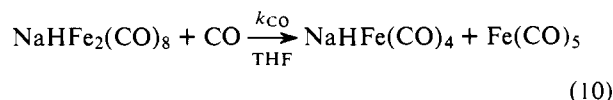
The addition of CO turns the red-brown $NaHFe_2(CO)_8$ solutions to a light yellow color characteristic of $NaHFe(CO)_4$ in THF; 1.0 ± 0.1 equiv of $CO/NaHFe_2(CO)_8$ was consumed and the only products observable by IR were $NaHFe(CO)_4$ and $Fe(CO)_5$. In measuring the [CO] dependence of the reduction of ethyl crotonate by $NaHFe_2(CO)_8$, the rate constant for CO cleavage of $NaHFe_2(CO)_8$ was also determined, k_{CO} (25.0 °C, constant CO pressure, $P_{CO} = 1$ atm, 0.088 M HOAc, THF) = 1.7×10^{-4} s⁻¹ (Table V, entry 11 and footnote i). This value for k_{CO} was independently verified by monitoring the uptake of CO volumetrically. The observed data, Figure 13, are reproduced reasonably well using the above value of k_{CO} and the known rates of $NaHFe_2(CO)_8$ decomposition. IR analysis of the product mixture showed that the known decomposition product $NaHFe_3(CO)_{11}$ (as well as $NaHFe(CO)_4$) was present, indicating that significant $NaHFe_2(CO)_8$ decomposition had occurred. It should be noted that the initial rate of the CO reaction, eq 10 under these conditions is about the same as the rate of CO(gas) → CO(solution), Figure 13.[43] Thus the concentration of free CO in these solutions is probably small.

Figure 14. Linear dependence of the initial rate upon the initial PPh_3 concentration for the reaction of $NaHFe_2(CO)_8$ and PPh_3 in THF with the initial $[NaHFe_2(CO)_8]$ constant.

Figure 15. Linear dependence of the initial rate upon the initial $NaHFe_2(CO)_8$ concentration for the reaction of $NaHFe_2(CO)_8$ and PPh_3 in THF with the initial $[PPh_3]$ constant.

In order to determine if a CO dissociative pathway, eq 11, was fast enough to be important in reductions using $NaHFe_2(CO)_8$, the exchange of ^{13}CO with $NaHFe_2(CO)_8$ was studied.

$$NaHFe_2(CO)_8 \underset{k_{-1}}{\overset{k_1}{\rightleftharpoons}} NaHFe_2(CO)_7 + CO \qquad (11)$$

Bubbling 20% ^{13}CO (1 atm, 25.0 °C, no HOAc present) through a 0.2 M $NaHFe_2(CO)_8$ solution for 3.0 min gave no detectable ^{13}CO incorporation by ^{13}C NMR. A ^{13}CO incorporation of $\geq 1.1\%$ would have been detected.[44] This ^{13}CO study requires the important result that $k_1 \leq 6 \times 10^{-5}\,s^{-1}$. The short, 3.0-min reaction time was required to prevent ^{13}CO cleavage of the iron–iron bond in $NaHFe_2(CO)_8$ (e.g., 10), which hampers the ^{13}C NMR analysis.[45] Under these conditions, only 2.8% of the CO-induced $NaHFe_2(CO)_8$ cleavage should have occurred. The presence of 1 equiv of *trans*-$CH_3CH{=}CHCO_2Et$ substrate did not catalyze the exchange of CO. No ^{13}CO incorporation was observed by ^{13}C NMR after 3.0 min of bubbling 20% ^{13}CO (1 atm, 25 °C) through a 0.2 M $NaHFe_2(CO)_8$/THF solution (no HOAc) that contained 0.2 M *trans*-$CH_3CH{=}CHCO_2Et$.

In order to study the ligand substitution mechanism of $NaHFe_2(CO)_8$ independent of the other processes involved in these reductions, the reaction of $NaHFe_2(CO)_8$ with ligands which cannot undergo the migratory insertion reaction, such as phosphines, was examined. The addition of PPh_3 to $NaHFe_2(CO)_8$ in THF results in iron–iron bond cleavage. The reaction of 2 equiv of $PPh_3/NaHFe_2(CO)_8$ in THF at 25.0 °C gives significant amounts of $NaHFe(CO)_4$, $Fe(CO)_3L_2$, $Fe(CO)_5$, some $Fe(CO)_4L$, but not $NaHFe(CO)_3L$ (L = PPh_3). The reaction stoichiometry, precise to $\pm 15\%$, is shown in eq 12.

$$1NaHFe_2(CO)_8 + 1L$$
$$(L = PPh_3)$$

$$\xrightarrow[\text{25.0 °C}]{\text{THF}} \quad [1NaHFe(CO)_4] + 0.4Fe(CO)_5$$
$$+ 0.4Fe(CO)_3L_2$$
$$\Big\downarrow H^+, L \quad + 0.2Fe(CO)_4L$$

$$H_2 + Fe(CO)_4L \qquad (12)$$

With 1 equiv of $HOAc/NaHFe_2(CO)_8$ present, the reaction of 2 equiv of $PPh_3/NaHFe_2(CO)_8$ gives a mixture of $Fe(CO)_5$, $Fe(CO)_4L$, and $Fe(CO)_3L_2$ (eq 12). However, the formation of more $Fe(CO)_4L$ occurs in a secondary reaction. In the presence of HOAc, $NaHFe(CO)_4$ and PPh_3 react to give H_2 and $Fe(CO)_4L$. By monitoring the disappearance of the IR

Figure 16. Linear dependence of the pseudo-first-order rate constant for $NaHFe_2(CO)_8$ decomposition upon the concentration of (excess) HOAc.

bridging carbonyl band of $NaHFe_2(CO)_8$ at 1770 cm^{-1}, kinetic data on the reaction of $NaHFe_2(CO)_8$ and PPh_3 have been obtained (Table IX). These data demonstrate that the disappearance of $NaHFe_2(CO)_8$ is overall second order, first order each in $[PPh_3]$ (Figure 14) and $[NaHFe_2(CO)_8]$ (Figure 15).

The observation of a second-order rate law and no isotope effect within experimental error, $k_H/k_D = 0.9 \pm 0.2$ (Table IX, entry 2, footnote *f*), for this reaction for important results which bear heavily upon possible mechanisms of reductions by $NaHFe_2(CO)_8$.

Further kinetic data show that this PPh_3 reaction is unaffected by added HOAc (Table IX, entry 6), but is slowed two- and threefold by adding 1 equiv of $NaHFe(CO)_4$ or crown ether/$NaHFe_2(CO)_8$, respectively (4 and 5). If the more nucleophilic phosphine $P(Ph)(CH_3)_2$ is used in place of PPh_3, the reaction is *at least* 30 times faster, $k_2 > 10^{-1}\,M^{-1}\,s^{-1}$.

Studies of $NaHFe_2(CO)_8$ Decomposition Mechanisms. In the synthetic reductions using $NaHFe_2(CO)_8$, it was observed that weak acids like NH_4Cl (Table 1, entry 8) often give higher yields of reduced carbonyl compound. The following data show that $NaHFe_2(CO)_8$ decomposes in the presence of acid. Monitoring the disappearance of the hydride resonance by ^1H NMR, the results summarized in Figure 16 show that $NaHFe_2(CO)_8$ decomposes by both a first-order acid-independent as well as a second-order acid-dependent pathway, k_1 (de-

Table IX. Kinetic Data for the Reaction of $NaHFe_2(CO)_8$ with PPh_3 (THF, 25.0 °C)

Entry	$[NaHFe_2(CO)_8] \times 10^2$, M	$[PPh_3]$, M	Other reagents	$k_1 \times 10^3$,[a,b] s^{-1}	$k_2 \times 10^3$,[c] $M^{-1} s^{-1}$
1	2.0, 4.0,[d] and 8.0	0.40			2.7
2	8.0	0.40,[e,f] 0.20			2.7
3	2.0	0.10[e]		0.32	3.2
4	8.0	0.20	0.08 M $NaHFe(CO)_4$ added	0.22	1.0
5	8.0	0.40	0.08 M dicyclohexyl-18-crown-6 added	0.46	1.4
6	8.0	0.40	0.088 M HOAc added	1.1	2.9

[a] k_1 = initial rate/initial $[NaHFe_2(CO)_8]$. The disappearance of $NaHFe_2(CO)_8$ was monitored by following the decrease in the IR absorbance of the bridging CO band at 1770 cm^{-1}. [b] For reactions with PPh_3 in excess, linear ln $[NaHFe_2(CO)_8]$ vs. time plots were usually obtained. For reactions with <4 equiv $PPh_3/Na_2Fe(CO)_8$, initial rates were used. (Linear $[NaHFe_2(CO)_8]^{1/2}$ vs. time plots were obtained.) [c] k_2 = k_1/initial $[PPh_3]$. [d] See Figure 15. [e] See Figure 14. [f] For 0.08 M $NaDFe_2(CO)_8$ and 0.4 M PPh_3, k_2 = 3.1 × 10^{-3} M^{-1} s^{-1}, and thus k_H/k_D = 0.9 ± 0.2 (error bars assuming ±15% in each rate constant).
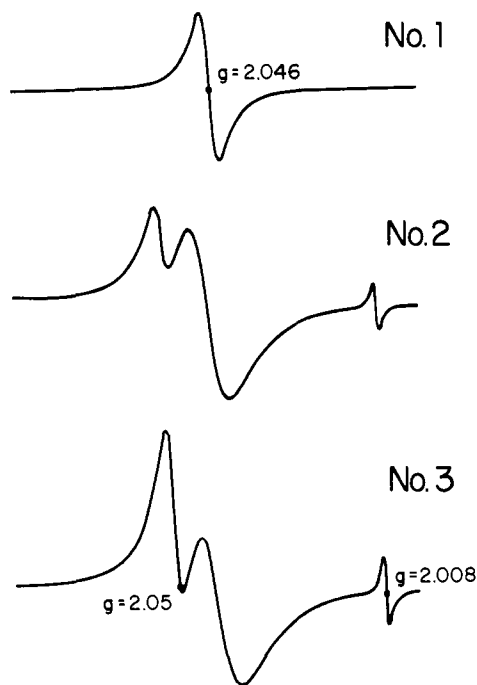
Figure 17. ESR (ambient temperature, THF) of (1) a typical 0.1 M $NaHFe_2(CO)_8$ solution; (2) a 0.1 M $NaHFe_2(CO)_8$ directly after addition of 0.18 M HOAc; (3) the reaction mixture of 0.10 M $NaHFe_2(CO)_8$ plus 0.20 M *trans*-CH_3CH=$CHCO_2Et$ (25.0 °C) 15 h after completion.

composition-total) = $k_{1D} + k_{2D}[HOAc]$, with k_{1D} = 2.3 × 10^{-5} s^{-1} and k_{2D} = 2.6 × 10^{-4} M^{-1} s^{-1} (25.0 °C). Thus with no HOAc present, $NaHFe_2(CO)_8$ decomposes with a $t_{1/2}$ = 8.4 h at 25 °C. In the presence of 0.2 M HOAc, this decomposition is accelerated to a $t_{1/2}$ of about 2.5 h. This instability of $NaHFe_2(CO)_8$ has made mechanistic studies of its chemistry considerably more difficult.

For the acid-independent path, the reaction stoichiometry is clearly[46] that depicted in the equation

$$3NaHFe_2(CO)_8 \rightarrow 2NaHFe(CO)_4 + 1NaHFe_3(CO)_{11} + 1Fe(CO)_5 \quad (13)$$
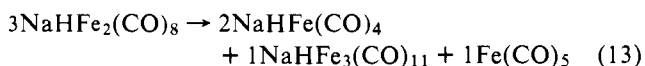
For the acid-catalyzed decomposition, increasing amounts of $NaHFe_3(CO)_{11}$ are observed by ^1H NMR with increasing [HOAc]. Using a large excess of HOAc (9 equiv HOAc/$NaHFe_2(CO)_8$), the products due solely to the acid-catalyzed $NaHFe_2(CO)_8$ decomposition could be observed. This stoichiometry, again established using ^1H NMR and GLC,[47] is shown in the equation

$$2NaHFe_2(CO)_8 + HX \rightarrow H_2 + NaHFe_3(CO)_{11} + Fe(CO)_5 + NaX \quad (14)$$
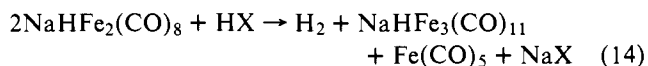
Added $NaHFe(CO)_4$ retards the first-order acid-independent $NaHFe_2(CO)_8$ decomposition path, but by only a factor of 2.6. (For 0.10 M $NaHFe(CO)_4$ and 0.10 M $NaHFe_2(CO)_8$, k_{1D}' = 8.6 × 10^{-6} s^{-1}, 25.0 °C.) Thus it appears that this pathway does not involve *reversible* iron–iron bond rupture to $NaHFe(CO)_4$ and $Fe(CO)_4$. The acid-independent path is also ion pairing insensitive relative to the reduction reactions. Added NMP (4.7% (v/v) NMP/THF) has no effect within experimental error, k_{1D}'' = 2.7 × 10^{-5} s^{-1} (25.0 °C).

ESR Detection of Radicals in $NaHFe_2(CO)_8$ Solutions. As stated previously, two reactions catalyzed by $NaHFe_2(CO)_8$/THF solutions have been observed that are possibly radical in nature. One is the incorporation of deuterium from $DFe_2(CO)_8^-$ into the allylic methyl group of CH_3CH=$CHCO_2Et$, eq 15, while the other is cis–trans isomerization without deuterium incorporation, eq 16.

$$CH_3CH=CHCO_2Et$$
$$\xrightarrow{"DFe_2(CO)_8^-"} CH_xD_{3-x}CH=CHCO_2Et \quad (15)$$

$$cis\text{-}CH_3CH=CHCO_2Et$$
$$\xrightarrow{"DFe_2(CO)_8^-"} trans\text{-}CH_3CH=CHCO_2Et \quad (16)$$

With the hope of observing directly possible free-radical species, ESR experiments were undertaken.

Spectrum 1, Figure 17, shows that in a typical 0.10 M $NaHFe_2(CO)_8$/THF solution, an ESR signal at g = 2.045 ± 0.002 is indeed seen at ambient temperature. No proton hyperfine is observed in this g = 2.046 signal. This signal is reminiscent of the g = 2.0455 (25 °C, THF) signal observed by Muetterties[18a] for the 17-electron, d^7, $C_3H_5Fe(CO)_3$ moiety:

$$[C_3H_5Fe(CO)_3]_2 \rightleftharpoons C_3H_5Fe(CO)_3 \cdot \quad (g = 2.0455) \quad (17)$$
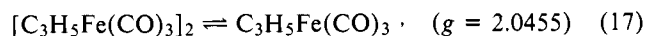
In order to test whether or not these radicals (Figure 17) are involved in reductions by "$NaHFe_2(CO)_8$", the following experiments were performed. These experiments were repeated and gave identical results each time.

In the first experiment, the addition of 0.18 M HOAc to a 0.1 M $NaHFe_2(CO)_8$/THF solution at 25 °C immediately gave an increase in the g = 2.046 signal along with new signals at g = 2.008 ± 0.002 and $g \simeq$ 2.05 (rigorously 2.046 < g < 2.055), spectrum 2, Figure 17. From the large magnitude of the g values, the two signals at $g \simeq$ 2.05 and g = 2.046 are undoubtedly transition metal free radicals while the smaller signal at g = 2.008 is an organic radical. Much smaller amounts of these same signals at $g \simeq$ 2.05 and g = 2.008 were observed in $NaHFe_2(CO)_8$/THF solution (no HOAc) that had been stored at 25 °C (under nitrogen) for about 6 h.

In the second experiment, the $g \simeq$ 2.05, 2.046, and 2.008 signals were monitored as a function of time during the re-

duction of *trans*-CH₃CH=CHCO₂Et. In the reaction of 0.10 M NaHFe₂(CO)₈ and 0.20 M *trans*-CH₃CH=CHCO₂Et, the signals at $g \simeq 2.05$ and 2.008 increased in intensity (the $g = 2.046$ signal remained approximately the same) at a rate similar to the rate of CH₃CH₂CH₂CO₂Et formation. Spectrum 3, Figure 17, shows the final ESR obtained after 18 h at 25 °C, about 15 h after all the CH₃CH=CHCO₂Et had been reduced. This spectrum shows that these radicals are quite stable. If these signals were due to reactive intermediates that are proportional to the concentration of NaHFe₂(CO)₈, they should have eventually disappeared.

Finally, additional experiments were designed to probe the identity and chemical reactivity of these radicals. The $g = 2.046$ signal is also observed in a saturated solution of Na₂Fe₂(CO)₈ in THF. Although this experiment makes it tempting to suggest that this signal is due to Na⁺(Fe(CO)₄)⁻, traces of water could protonate this species to give HFe(CO)₄. A very weak $g = 2.046$ signal is also observed in solutions of NaHFe(CO)₄ and Et₃NH⁺(HFe₃(CO)₁₁)⁻. Although a 0.10 M NaHFe₂(CO)₈ in THF solution did not initiate the polymerization of 0.40 M styrene, addition of dimethyl maleate immediately removed the $g = 2.056$ signal, but did not affect the $g = 2.046$ or 2.008 signals.

Mechanistic Studies of Reductions in 1,4-Dioxane Using Na₂Fe(CO)₄, Fe(CO)₅, and HOAc. The insolubility of NaHFe₂(CO)₈ and NaHFe(CO)₄ in dioxane has severely thwarted attempts[48a] to discover the active reagent(s) in this solvent, and no definitive conclusions about the active species(s) can be reached.[48b]

Mechanistic Studies of HFe(CO)₄⁻ Additions to α,β-Unsaturated Carbonyl Compounds. In order to be able to compare them directly to reduction using binuclear NaHFe₂(CO)₈, additions of mononuclear NaHFe(CO)₄ to α,β-unsaturated carbonyl compounds were briefly examined. As mentioned previously, eq 6, the addition of NaHFe(CO)₄ to CH₂=CHCO₂Et is regiospecific and irreversible, yielding an isolable α-iron alkyl intermediate, [CH₃CH(Fe(CO)₄)CO₂Et]⁻. This reaction is inhibited by *at least* 100-fold by 1 atm of CO, a result also observed by Takegami.[49]

At 25.0 °C, bubbling 20% ¹³CO (1 atm CO with no HOAc present) through a 0.2 M NaHFe(CO)₄ solution in THF showed on the average that 3.6% of the four carbonyls in NaHFe(CO)₄ had exchanged in 3.0 min by ¹³C NMR analysis.[50] These ¹³CO incorporation and CO inhibition studies are consistent with the active species being the coordinatively unsaturated hydride, NaHFe(CO)₃:

$$\text{NaHFe(CO)}_4 \underset{k_{-1}'}{\overset{k_1'}{\rightleftharpoons}} \text{NaHFe(CO)}_3 + \text{CO} \qquad (18)$$

Thus in 3.0 min, at least 14% of the NaHFe(CO)₄ ($K_1' \simeq 9 \times 10^{-4}$ s⁻¹) gives NaHFe(CO)₃ + CO.

It is important to note that in order for the NaHFe(CO)₄ and NaHFe₂(CO)₈ ¹³CO exchange results to be directly comparable, they were run side by side, under identical conditions. As stated previously, NaHFe₂(CO)₈ showed no ¹³CO incorporation in 3.0 min, requiring $k_1 \leq 6 \times 10^{-5}$ s⁻¹ (eq 11).

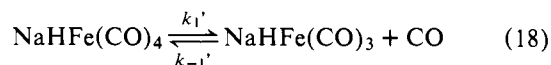Since monoiron alkyl compounds, RFe(CO)₄⁻, are the primary product of NaHFe₂(CO)₈ additions in the absence of acid to α,β-unsaturated carbonyl compounds, their protonolysis reaction to yield RH was briefly studied. Previously, addition of 0.16 M HOAc to 0.1 M Na⁺[CH₃CH₂CH(Fe(CO)₄)CO₂Et]⁻ gave complete protonolysis to CH₃CH₂CH₂CO₂Et in ≤1 min at 25.0 °C, $k_2 \geq 0.07$ M⁻¹ s⁻¹. Monitoring the reaction by ¹H NMR, a 0.12 M solution of previously isolated[37] PPN⁺[CH₃CH(Fe(CO)₄)CO₂Et]⁻ in THF-d_8 and 0.22 M HOAc gave a reasonable fit to a second-order plot with $k_2 \sim 9 \times 10^{-3}$ M⁻¹ s⁻¹ at 35 °C. The reaction rate of an identical experiment except with ~five times

as much HOAc was approximately five times faster. Usually the protonolysis of RFe(CO)₄⁻ compounds (R = *n*-alkyl) is very fast.[29] Thus it appears that α-electron withdrawing ester groups stabilize the alkyl iron compounds and reduce the rate of protonolysis. Also, it tentatively appears that there is an ion-pairing effect upon this protonolysis since the Na⁺ salt is faster than the PPN⁺ salt even though the PPN⁺ reaction was carried out at 35 °C, 10 °C higher than the Na⁺ reaction. We presume that this protonolysis proceeds via a sequence at iron of oxidative addition of H⁺, followed by reductive elimination of RH.

Discussion

Synthetic. A comparison of various common methods used to reduce the olefinic bond in α,β-unsaturated carbonyl compounds is given in Table X. The reductions described in this paper utilizing NaHFe₂(CO)₈ or Na₂Fe(CO)₄, Fe(CO)₅, and HOAc in dioxane can be seen to be superior to or to complement the other available methods that effect this transformation.

Noyori[51] has described a related reduction based on Fe(CO)₅ and NaOH in methanol. Although the active species is not defined by Noyori, experiments in our laboratory have demonstrated that initially NaHFe(CO)₄ is the only iron hydride formed under his conditions. Reductions of Δ¹,⁹-2-octalone yield products with a cis/trans ratio of 37/63 under Noyori's conditions,[65] while NaHFe₂(CO)₈ gives cis/trans = 4/1 (entry 6, Table I) and the dioxane conditions give cis/trans = 87/13 (entry 2, Table II). Both in dioxane as well as THF, reductions using NaHFe₂(CO)₈ are faster and give higher yields.

Both sets of reducing conditions described in this paper are specific to double bonds conjugated to carbonyl groups, as demonstrated by the reduction of carvone (entry 3, Table I, and entry 1, Table II). This is in contrast to Wilkinson's catalyst (entry 7, Table X), which preferentially hydrogenates the isopropenyl group in this substrate. The very promising hydrosilylation techniques (entry 8, Table X) developed by Ojima[56] is also specific for conjugated double bonds. Isolated double bond attack is a problem with a number of other reducing methods (10, 14, 15).

Although heterogeneous hydrogenation suffers from many problems, including selectivity,[55a] conditions are available for the reduction of olefins conjugated to carbonyl groups in the presence of isolated double bonds.[62c] Heterogeneous hydrogenation conditions exist[62a] for the reduction of Δ¹,⁹-2-octalone with cis/trans = 93/7, which is better than the 87/13 ratio achieved in this paper (entry 2, Table II). Heterogeneous hydrogenation has an advantage over homogeneous transition metal systems in that it is better at reducing large, bulky substrates like steroids. Homogeneous systems have the advantage of greater selectivity and mildness, as demonstrated by the toleration of epoxides, amides, nitriles, lactones, and aldehydes by NaHFe₂(CO)₈.

Dissolving metal reductions (15) are particularly useful for the reductions of enones in steroids.[63d] In fused ring systems, low cis/trans ratios are usually obtained,[63a,d] in contrast to the reductions described in this paper. For simpler substrates, dimerization is a problem, although it can be diminished by addition of a proton donor.[62e,f]

Mechanistic. Previously,[21a] we presented preliminary evidence for the mechanism of reductions using NaHFe₂(CO)₈ in THF shown in Scheme II. We now consider this mechanism step by step, with the corresponding evidence bearing on each step.

The First Step. The first step, concerted reaction of the olefin with NaHFe₂(CO)₈, was postulated after the four plausible, a priori, NaHFe₂(CO)₈ fragmentation reactions, Scheme III,

Table X. Methods for Reducing the Olefinic Bond in α,β-Unsaturated Carbonyl Compounds

Entry	Reagent	Types of α,β-unsaturated compds reduced	Advantages	Disadvantages	Ref
1	$NaHFe_2(CO)_8$	Aldehydes, ketones, esters, lactones, amides, nitriles	Mild, selective, high yield	Stoichiometric, air sensitive	
2	$Na_2Fe(CO)_4$, $Fe(CO)_5$, HOAc, dioxane	Ketones, esters, nitriles	Selective, high yield	Stoichiometric, air sensitive, reduces aldehydes	
3	$Fe(CO)_5$, NaOH	Aldehydes, ketones, esters, lactones, nitriles	Mild, high yield	Stoichiometric, air sensitive, slow reactions	51
4	$HCo(CO)_4$	Ketones, aldehydes		Stoichiometric, high temp and pressure required to generate $HCo(CO)_4$, limited to simple substrates, reduction under CO atmosphere required	52
5	$HCo(CN)_5^{3-}$	Ketones, esters, acids, amides, nitriles	Catalytic	Aldehydes are reduced slowly	53
6	LiCuHR	Ketones, aldehydes, esters	Selective	Greater than 4 equiv of the hydride required, substrates polymerize in some cases, air sensitive	54
7	RhL_3Cl	Ketones, aldehydes, esters, acids, nitro compounds	Catalytic selective	CO abstracted from aldehydes, reductions air sensitive	55
8	RhL_3Cl, R_3SiH	Ketones, aldehydes	Catalytic, high yield, selective	Nitriles give stable α-silyl nitriles, reductions air sensitive	56
9	$Rh_6(CO)_{16}$, CO, H_2O, $Rh_4(CO)_{12}$	Ketones, aldehydes, nitriles, amides	Catalytic selective	High pressure required	57
10	RuL_3Cl_2, alcohol	Ketones	Catalytic	Rearranges carvone, reductions air sensitive	58
11	$CrCl_2$	Esters, acids, nitriles, ketones	Olefins not isomerized	Limited primarily to substrates activated by two carbonyls	59
12	$NaBH_4$	Esters, nitriles, amides lactones	Readily available	Limited primarily to substrates activated by two carbonyls	60
13	$PhCH_2NH_2KOBu$-t	Ketones	Readily available	Yields for some simple ketones are low	61
14	Heterogeneous hydrogenation	Ketones, esters, aldehydes, nitriles	Catalytic	Lack of selectivity, double bond migration	62, 55a
15	Dissolving metal reductions	Ketones, esters, acids	Readily available	Reductive coupling to dimers; may reduce terminal nonconjugated double bonds	63
16	Zn, HCl	Ketones	Readily available	Causes skeletal rearrangements	64

were tested and found inconsistent with the experimental results. In fact, the observation of a rate law first order each in $NaHFe_2(CO)_8$ and $RCH=CHCOR'$ rules out *any* mechanism (such as a–d, Scheme III) where $NaHFe_2(CO)_8$ reversibly breaks up into two fragments, only one of which eventually reacts with $RCH=CHCOR'$. Such mechanisms would show rate laws $\alpha[NaHFe_2(CO)_8]^{1/2}[RCH=CHCOR']^1$. If the fragmentation were irreversible, it would show a rate law for α $[NaHFe_2(CO)_8]^1$ $[RCH=CHCOR']^0$. This conclusion is verified by our independent study of the PPh_3 ligand substitution mechanism of $NaHFe_2(CO)_8$, which also shows a rate law first order in each reactant. The fact that reductions using $NaHFe_2(CO)_8$ are not inhibited by added $Fe(CO)_5$ and the observation that $NaHFe_2(CO)_8$ is *at least* 26 times more reactive than $NaHFe(CO)_4$ confirms that fragmention reactions (b) and (c), respectively, followed by reaction of only one of the fragments with $RCH=CHCOR'$ are not involved. However, other mechanisms involving $NaHFe_2(CO)_8$ fragmentation can be written that are consistent with the observed kinetics, first order each in $NaHFe_2(CO)_8$ and $RCH=CHCOR'$. In general, these fragmentation–recombination mechanisms[66] involve reversible breakup of $NaHFe_2(CO)_8$ into two fragments, A + B, the reversible reaction of one of the fragments, presumably the coordinatively unsaturated one, with $RCH=CHCOR'$, to give a new fragment B', followed by the reversible reaction of A with B' to generate some intermediate such as II, Scheme II. Also possible is reaction between $NaHFe_2(CO)_8$ and $RCH=CHCOR'$ to give A + B' directly. A mechanistic feature of all of the fragmentation recombination mechanisms is that they are multistep ways to accomplish what step 1, Scheme II, accomplishes in a single step. A variety of experiments were designed to test these possible mechanisms and are presented below. We feel that these data, especially the consideration of the PPh_3 ligand substitution reaction, suggest that any such

fragmentation–recombination mechanism involving reactions (a–d), Scheme III, are unlikely to be important.

The participation of reactions (b) or (c) both in reductions using $NaHFe_2(CO)_8$ and its reaction with PPh_3 has been ruled out by several pieces of evidence. The fact that $NaHFe(CO)_3L$ (L = PPh_3) is not formed in the reaction of $NaHFe_2(CO)_8$ with PPh_3 argues against any fragmentation–recombination mechanism involving the formation of $NaHFe(CO)_3$ or the direct reaction of olefin with $NaHFe_2(CO)_8$ to give $NaHFe(CO)_3$(olefin) as a first step. Fragmentation–recombination mechanisms involving $NaHFe(CO)_4$ and $Fe(CO)_4$, reaction (c), can also be ruled out by our studies of the PPh_3 substitution reaction. If fragmentation to $NaHFe(CO)_4$ + $Fe(CO)_4$ were important, then the PPh_3 ligand substitution products should be $NaHFe(CO)_4$ + $Fe(CO)_4(L)$. For example, $Fe(CO)_4$-(olefin) plus 1 equiv of PPh_3 react, via initial olefin dissociation, to give a predominantly $Fe(CO)_4(PPh_3)$ but, as is often observed,[81,82] also some $Fe(CO)_3(PPh_3)_2$ with a $Fe(CO)_3$-$(PPh_3)_2/Fe(CO)_4(PPh_3)$ ratio $\ll 1/3$. In contrast, we observe mostly $Fe(CO)_3(PPh_3)_2$ with a $Fe(CO)_3(PPh_3)_2/Fe(CO)_4$-$(PPh_3)$ ratio of 2. Furthermore, a control reaction demonstrated that $Fe(CO)_4(PPh_3)$ is stable under the reaction conditions. Authentic $NaHFe(CO)_4$, $Fe(CO)_4(PPh_3)$, and PPh_3 showed no observable further reaction (i.e., to $Fe(CO)_3$-$(PPh_3)_2$) in 4 h. The above results argue against fragmentation–recombination mechanisms involving $NaHFe(CO)_4$ and $Fe(CO)_4$. However, we note that for PPh_3, its direct reaction with $NaHFe_2(CO)_8$ to give $NaHFe(CO)_4$ and $Fe(CO)_4$-(PPh_3) appears to be a viable pathway (vide infra, Scheme IV). Thus we can postulate a sequence of steps in which olefin reacts reversibly with $NaHFe_2(CO)_8$ to produce $NaHFe(CO)_4$ plus $Fe(CO)_4$(olefin) followed by efficient, reversible recombination of these fragments to give II, Scheme II. Indeed, mixing 1 equiv each of $NaHFe(CO)_4$, $Fe(CO)_4(PhCH=CHCO_2Et)$, and HOAc produces essentially the same results

Scheme II. Proposed Mechanism for the Reduction of $RCH=CHCOR'$ by $NaHFe_2(CO)_8$

$$NaHFe_2(CO)_8$$
$$\mathbf{I}$$
$$+$$
$$RCH=CHCOR' \underset{k_{-1}}{\overset{k_1}{\rightleftharpoons}} Na^+ \left[\begin{array}{cc} RCH-CHCOR' \\ | \quad\quad | \\ H \quad Fe_2(CO)_8 \end{array} \right]^-$$

$$\mathbf{II}$$

$$Na^+ \left[\begin{array}{cc} RCH-CHCOR' \\ | \quad\quad | \\ H \quad Fe_2(CO)_8 \end{array} \right]^- \overset{k_2}{\longrightarrow} Na^+ \left[\begin{array}{c} RCH_2CHCOR' \\ | \\ Fe(CO)_4 \end{array} \right]^-$$

$$\mathbf{II} \qquad\qquad\qquad\qquad\qquad \mathbf{III}$$
$$+$$
$$Fe(CO)_4$$

$$\mathbf{II} \overset{k_3}{\underset{HX}{\searrow}}$$

$$RCH_2CH_2CO_2R' + Fe_2(CO)_8 + NaX$$

Reactions Occurring after the Rate-Determining Step

$$Na^+ \left[\begin{array}{c} RCH_2CHCOR' \\ | \\ Fe(CO)_4 \end{array} \right]^- + HX$$

$$\overset{fast}{\longrightarrow} RCH_2CH_2COR' + Fe(CO)_4 + NaX$$

$$2Fe(CO)_4 \overset{fast}{\longrightarrow} Fe_2(CO)_8$$

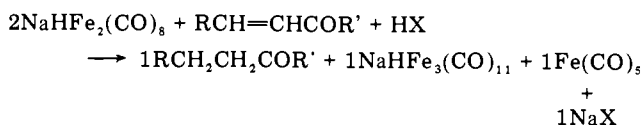$$Fe_2(CO)_8 + NaHFe_2(CO)_8 \overset{fast}{\longrightarrow} NaHFe_3(CO)_{11} + Fe(CO)_5$$
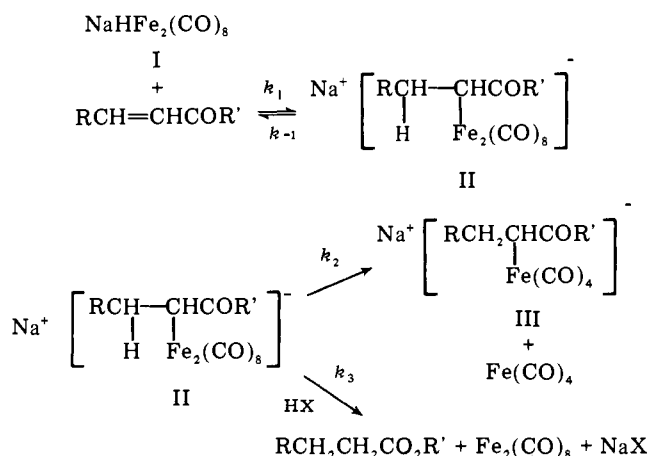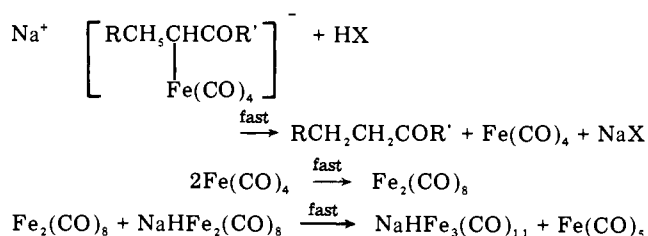
Predicted Stoichiometries

With HOAc

$$2NaHFe_2(CO)_8 + RCH=CHCOR' + HX$$
$$\longrightarrow 1RCH_2CH_2COR' + 1NaHFe_3(CO)_{11} + 1Fe(CO)_5$$
$$+$$
$$1NaX$$

Without HOAc

$$3NaHFe_2(CO)_8 + 2RCH=CHCOR'$$
$$\longrightarrow 2Na[RCH_2CH(Fe(CO)_4)COR'] + 1NaHFe_3(CO)_{11}$$
$$+$$
$$1Fe(CO)_5$$
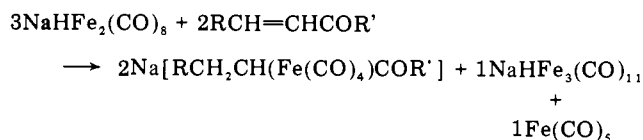
Predicted Kinetic Expression $(K_1 \ll 1)$

$$\frac{d[RCH_2CH_2COR']}{dt}$$

$$= K_1(k_2 + k_3[HX])[NaHFe_2(CO)_9][RCH=CHCOR']$$

Observed Kinetic Expression

$$\frac{d[RCH_2CH_2COR']}{dt}$$

$$= (k_{2R} + k_{3R}[HX])[NaHFe_2(CO)_8][RCH=CHCOR']$$

as starting the reaction with $NaHFe_2(CO)_8$ and $PhCH=CHCO_2Et$. At present, we cannot rule out this possibility, but have simply chosen the least complex mechanism, Scheme IV.

A CO dissociative pathway, reaction (a), was initially what we expected $NaHFe_2(CO)_8$ and other systems with bridging carbonyls to exhibit. A recent study[10a] of the ligand substitution reactions of $Ir_4(CO)_{12}$ provides excellent precedent for this hypothesis. However, the lack of facile ^{13}CO exchange with $NaHFe_2(CO)_8$, $k_{1a} \le 6 \times 10^{-5}$ s^{-1} (Scheme III), and the small CO dependence of these reductions are inconsistent with a CO dissociative pathway. Furthermore, the unexpected,[68] yet facile ^{13}CO exchange with $NaHFe(CO)_4$ (under identical conditions) and the large CO dependence of NaH-

Scheme III. Plausible, a Priori, $NaHFe_2(CO)_8$ Fragmentation Reactions

$$NaHFe_2(CO)_8 \begin{array}{l} \overset{k_{1a}}{\underset{k_{-1a}}{\rightleftharpoons}} NaHFe_2(CO)_7 + CO \qquad (a) \\ \overset{k_{2a}}{\underset{k_{-2a}}{\rightleftharpoons}} NaHFe(CO)_3 + Fe(CO)_5 \quad (b) \\ \overset{k_{3a}}{\underset{k_{-3a}}{\rightleftharpoons}} NaHFe(CO)_4 + Fe(CO)_4 \quad (c) \\ \overset{k_{4a}}{\underset{k_{-4a}}{\rightleftharpoons}} HFe(CO)_4\cdot + Na^+(Fe(CO)_4)^{-}\cdot \quad (d) \end{array}$$
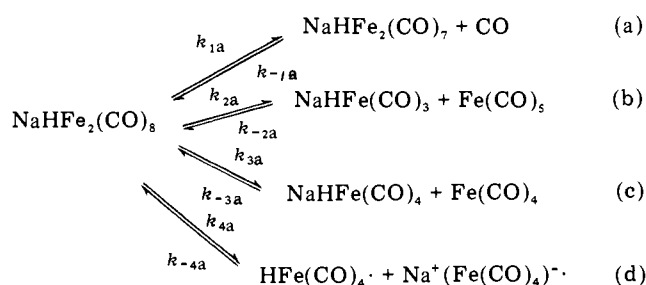
$Fe(CO)_4$ reductions emphasizes the difference between the $NaHFe_2(CO)_8$ mechanism and the $NaHFe(CO)_4$ CO dissociative mechanism. The fact that added trans-$CH_3CH=CHCO_2Et$ does not catalyze the exchange of ^{13}CO with $NaHFe_2(CO)_8$ rules out an associative CO displacement by $CH_3CH=CHCO_2Et$. As final proof for the fact that free CO cannot be involved in these reductions, $NaHFe(CO)_4$ is never seen as a product of reductions using $NaHFe_2(CO)_8$. Free CO and $NaHFe_2(CO)_8$ react rapidly to form $NaHFe(CO)_4$ and $Fe(CO)_5$.

The final possible fragmentation–recombination mechanism involves the radicals $HFe(CO)_4\cdot$ and $Fe(CO)_4^-\cdot$, reaction (d). In the presence of acid, protonation of $HFe_2(CO)_8^-$ to give $H_2Fe_2(CO)_8$ followed by its fragmentation to $HFe(CO)_4\cdot$ could occur (eq 19), consistent with the observed acid dependence.

$$HFe_2(CO)_8^- + H^+ \rightleftharpoons H_2Fe_2(CO)_8 \rightleftharpoons 2HFe(CO)_4\cdot \quad (19)$$
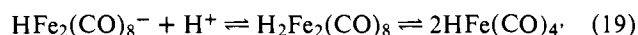
This reaction has some precedent in that rapid fragmentation at 25 °C of the formally d^7 binuclear iron system, $[C_3H_5Fe(CO)_3]_2$, to give reactive $C_3H_5Fe(CO)_3\cdot$ monomers, has recently been observed.[18a] However, it is interesting to note that this system has an extremely long Fe–Fe bond,[70] 3.13 Å, while $HFe_2(CO)_8^-$ is apparently held together more tenaciously, the Fe–Fe distance[24] being 2.521 Å. This shorter bond distance is consistent with the general observation[71] that bridging carbonyls reduce the metal-metal bond distance (although bridging hydrides often increase it about 0.15 Å[72]).

If one writes a mechanism using the reaction of d^6, $HCo^{III}(CN)_5^{3-}$ with α,β-unsaturated carbonyl compounds as a model[73] and keeping in mind the observed kinetics, one would expect $HFe(CO)_4\cdot$ and $RCH=CHCOR'$ to react via hydrogen atom transfer to give the free radical $RCH_2\dot{C}HCOR'$ and $Fe(CO)_4$ (eq 20), consistent with our observed regiospecificity.

$$RCH_2CH_2COR' + Fe(CO)_4$$
$$\uparrow HFe(CO)_4\cdot$$
$$HFe(CO)_4\cdot + RCH=CHCOR' \rightleftharpoons RCH_2\dot{C}HCOR' + Fe(CO)_4$$
$$\downarrow Fe(CO)_4^-\cdot$$
$$[RCH_2CH(Fe(CO)_4)COR']^-$$

$$(20)$$
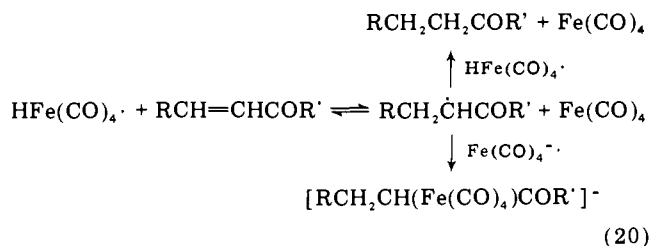
As expected for a radical mechanism, reductions with $HCo(CN)_5^{3-}$ show radical-dimerization products and that methyl substitution α to the carbonyl greatly increase the reaction rate owing to stabilization of the resultant organic radical. Also, $HCo(CN)_5^{3-}$ will initiate polymerization reactions. *Exactly the opposite results are found for NaHFe$_2$(CO)$_8$.* High, often 100%, yields of reduced product, RCH_2CH_2COR', but no dimers are observed. α-Methyl substitution slows the rate of reduction and $NaHFe_2(CO)_8$ in

Scheme IV. Proposed Mechanism for NaHFe$_2$(CO)$_8$ Ligand Substitution Reactions

$$\text{NaHFe}_2(\text{CO})_8 + \text{L} \underset{k_2}{\overset{k_1}{\rightleftharpoons}} \begin{cases} \text{NaHFe(CO)}_4 + \text{Fe(CO)}_4\text{L} \\ \text{NaHFe}_2(\text{CO})_7(\text{L}) + \text{CO} \end{cases}$$

Reactions Occurring after the Rate-Determining Step

$$\text{NaHFe}_2(\text{CO})_7(\text{L}) \begin{cases} \xrightarrow{\text{L}} \text{NaHFe(CO)}_4 + \text{Fe(CO)}_3\text{L}_2 \\ \xrightarrow{\text{CO}} \text{NaHFe(CO)}_4 + \text{Fe(CO)}_4\text{L} \end{cases}$$

$$\text{CO} + \text{NaHFe}_2(\text{CO})_8 \rightarrow \text{NaHFe(CO)}_4 + \text{Fe(CO)}_5$$
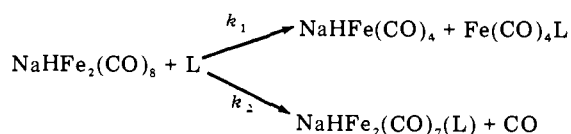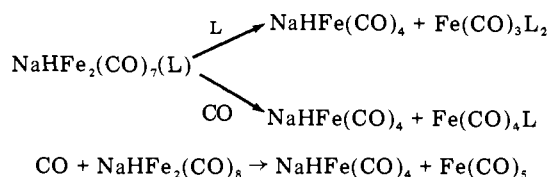
THF will not initiate the polymerization of styrene. Also, this mechanism (eq 20) could easily deviate from the simple kinetics observed, rate $\alpha[\text{NaHFe}_2(\text{CO})_8]^1[\text{RCH}=\text{CHCOR}']^1$, and it is unlikely that the hydrogen atom transfer from HFe(CO)$_4$· to RCH=CHCOR' would be reversible as required by our data or would show our inverse deuterium isotope effect. In fact, because of the fact that the reaction HFe(CO)$_4$· + RCH$_2$ĊHCOR' → RCH$_2$CH$_2$COR' + Fe(CO)$_4$ would be rate determining, this radical mechanism should show a positive primary deuterium isotope effect. It also appears that the radicals we observed by ESR are not involved in these reduction reactions.[74] Finally, the stereospecificity we see in deuterium isotope labeling studies using cyclic substrates such as 4,4-dimethylcyclohexenone is inconsistent with reversible formation of a RCH$_2$ĊHCOR' free radical. On the basis of the above arguments, we disfavor fragmentation-recombination mechanisms involving HFe(CO)$_4$· or HFe(CO)$_4$· and Fe(CO)$_4^-$·.

At this point, we have considered all plausible NaHFe$_2$(CO)$_8$ fragmentation reactions. The simplest interpretation of these results is that the first step involves concerted addition of NaHFe$_2$(CO)$_8$ to RCH=CHCOR', step 1, Scheme II. Previously,[21a] since most organometallic reactions occur in discrete, simple steps, we invoked a step involving associative olefin coordination to give NaHFe$_2$(CO)$_8$(RCH=CHCOR'), a species which appears to violate the 18-electron rule. Although structures can be written[75] for this species that do not violate the 18-electron rule, we have omitted this possible intermediate since a careful IR and low-temperature ^{13}C and 100-MHz NMR search provided no evidence for its existence. Initial electron transfer to give [HFe$_2$(CO)$_8$· + RĊHCH=C(O$^-$)R'] is also consistent with our data, even though no correlation was observed between the k_2(obsd) vs. the $E_{1/2}$ reduction potential of various substrates. Even if the first step involved electron transfer, such a correlation is unlikely since reductions using NaHFe$_2$(CO)$_8$ are sensitive to steric effects and because electron transfer would not be the rate-determining step.

It may be recalled that we cannot rule out a fragmentation-recombination mechanism involving direct reaction of NaHFe$_2$(CO)$_8$ and olefin to give NaHFe(CO)$_4$ + Fe(CO)$_4$(olefin) followed by their efficient, reversible recombination. *An important result of this work is that if this or other fragmentation-recombination mechanisms are involved, the recombination reaction is very efficient. Thus the fragments formed*[75] *are not "free", but behave as "caged" or "paired" fragments.*

Reversible, regiospecific hydride addition, I ⇌ II (Scheme II), is required by our deuterium isotope labeling studies and our inverse isotope effect. We have shown that the observed inverse isotope effect could be quantitatively accommodated by this equilibrium. In short, this equilibrium isotope effect is inverse because the zero-point energy difference between a

(bridging) Fe$_2$-H and Fe$_2$-D bond is less than that between a C-H and C-D bond. This appears to be the most reasonable way to account for this inverse isotope effect.[78b] Although we attempted to generate II (and thus III) independently by the addition of CH$_3$CH$_2$CH(OTs)CO$_2$Et to Na$_2$Fe$_2$(CO)$_8$ in THF-d_8, no identifiable products were observed by NMR.

The Remaining Steps. After the initial part of this mechanism is established, the remaining steps follow quite naturally.

In the next step, the alkyl intermediate, [RCH$_2$CH(Fe$_2$(CO)$_8$)COR']$^-$ (II), is partitioned between two paths. In the absence of acid iron-iron bond cleavage to the stable mononuclear [RCH$_2$CH(Fe(CO)$_4$)COR']$^-$ (III), and Fe(CO)$_4$ is the rate-determining step (III was observed directly by NMR). When HOAc is present, protonolysis of II occurs. The presence of these two pathways is required by the HOAc dependence, k_2(obsd) = $k_{2R} + k_{3R}$[HOAc]. Note that only at approximately 0.10 M HOAc do these pathways compete equally, i.e., $k_{2R}/(k_{3R}[\text{HOAc}]) \approx 0.1$ M/[HOAc].

After the rate-determining step, three reactions occur. First, the protonolysis of III occurs. This was studied independently and found to be fast as required by the reduction reaction kinetics. Next Fe(CO)$_4$ dimerizes to Fe$_2$(CO)$_8$. This reaction has been observed for Fe(CO)$_4$ generated in a matrix.[80] Interestingly, the formation of Fe$_2$(CO)$_8$ can account[81] for the presence of Fe(CO)$_3$L$_2$ (L = PR$_3$) when Fe(CO)$_4$ is generated in the presence of L. The formation of Fe(CO)$_3$L$_2$ was studied previously but is not well understood.[82] The third reaction is capture of Fe$_2$(CO)$_8$ by NaHFe$_2$(CO)$_8$ to give NaHFe$_3$(CO)$_{11}$ + Fe(CO)$_5$. This reaction has been observed independently in the acid-catalyzed NaHFe$_2$(CO)$_8$ decomposition mechanism. It is this step which accounts for the greater than 1 NaHFe$_2$(CO)$_8$/RCH=CHCOR' stoichiometry.

As shown in Scheme II, this mechanism accounts quite nicely for the observed stoichiometry and kinetics both with and without HOAc.

Ion Pairing. These studies demonstrate that triple ions, tight and solvent-separated ion pairs, as well as dissociated ions are formed by NaHFe$_2$(CO)$_8$ in THF. In addition, the Na$^+$ cation prefers to bind to the bridging vs. the terminal carbonyl groups. A rate decrease is observed for Li$^+$ > Na$^+$ > PPN$^+$ > Na$^+$-(crown) > Na$^+$·(5.2NMP) although the total rate span is only a factor of 7. Although it is clear that dissociated and solvent-separated ions are less reactive, the exact contributions by tight vs. triple ions cannot be determined from our data.

Comparison of HFe$_2$(CO)$_8^-$ and HFe(CO)$_4^-$ Mechanisms. A comparison of the mechanisms of the binuclear vs. the mononuclear hydride reveals several interesting points. First, HFe$_2$(CO)$_8^-$ has an associative first step whereas HFe(CO)$_4^-$ is dissociative. Second, HFe$_2$(CO)$_8^-$ exhibits a reversible migratory insertion while that of HFe(CO)$_4^-$ is irreversible. Third, the protonolysis of RFe$_2$(CO)$_8^-$ to yield RH is relatively slow whereas RFe(CO)$_4^-$ reacts rapidly with a proton to give RH. It is likely that the comparison of other binuclear and higher clusters to their mononuclear counterparts will reveal further differences.

PPh$_3$ Substitution. Eventual iron-iron bond cleavage is the predominant reaction of HFe$_2$(CO)$_8^-$ and added ligands such as CO or PPh$_3$. The first step of these reactions must be associative to account for the second-order rate law, rate α·[NaHFe$_2$(CO)$_8$]^1[PPh$_3$]^1, the small value of $k_H/k_D = 0.9 \pm 0.2$, the products (especially Fe(CO)$_3$PPh$_3$)$_2$[83]) and stoichiometry observed, and the fact that all plausible fragmentation of fragmentation-recombination mechanisms (reactions (c-d), Scheme II) have been ruled out. The mechanism proposed for PPh$_3$ substitution, Scheme IV, is supported by all our observations. From the ratio of Fe(CO)$_4$L/Fe(CO)$_3$L$_2$ of ≃½ we conclude that $k_1/k_2 \simeq$ ½. The small isotope effect observed,

Scheme V. Proposed Mechanisms for NaHFe₂(CO)₈
Acid-Independent and Acid-Dependent Decomposition

Without Acid

$$\text{NaHFe}_2(\text{CO})_8 \xrightarrow[\text{rds}]{k_{1D}} \text{NaHFe}(\text{CO})_4 + \text{Fe}(\text{CO})_4$$

$$\text{Fe}(\text{CO})_4 \xrightarrow{\text{fast}} {}^1\!/_2\,\text{Fe}_2(\text{CO})_8$$

$$\text{Fe}_2(\text{CO})_8 + \text{NaHFe}_2(\text{CO})_8 \xrightarrow{\text{fast}} \text{NaHFe}_3(\text{CO})_{11} + \text{Fe}(\text{CO})_5$$

Sum

$$3\text{NaHFe}_2(\text{CO})_8 \rightarrow 2\text{NaHFe}(\text{CO})_4$$
$$+ 1\text{NaHFe}_3(\text{CO})_{11} + 1\text{Fe}(\text{CO})_5$$

With Acid

$$\text{NaHFe}_2(\text{CO})_8 + \text{HX} \underset{}{\overset{k_1}{\rightleftharpoons}} \text{H}_2\text{Fe}_2(\text{CO})_8 + \text{NaX}$$

$$\xrightarrow[\text{rds}]{k_2} \text{H}_2 + \text{Fe}_2(\text{CO})_8$$

$$\text{Fe}_2(\text{CO})_8 + \text{NaHFe}_2(\text{CO})_8 \xrightarrow{\text{fast}} \text{NaHFe}_3(\text{CO})_{11} + \text{Fe}(\text{CO})_5$$

Sum

$$2\text{NaHFe}_2(\text{CO})_8 + \text{HX} \rightarrow \text{H}_2 + \text{NaHFe}_3(\text{CO})_{11}$$
$$+ \text{Fe}(\text{CO})_5 + \text{NaX}$$
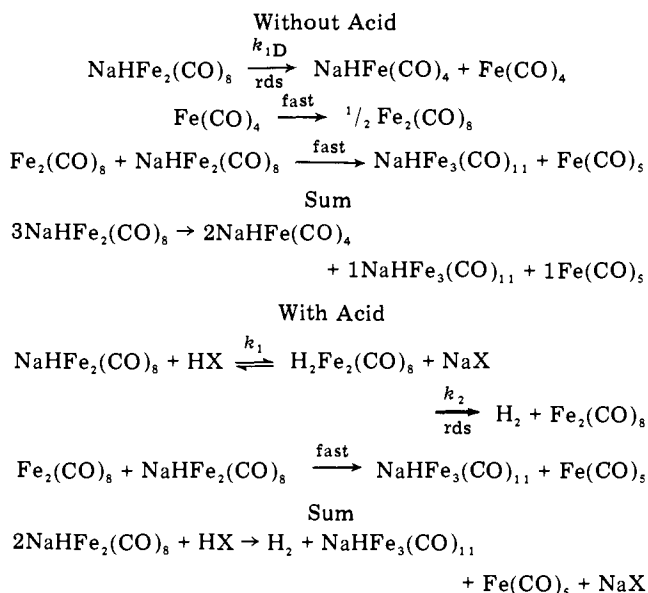
$k_H/k_D = 0.9 \pm 0.2$, in the reaction with PPh₃, a ligand that cannot undergo migratory insertion, strongly supports our assertion that the inverse isotope effect in reduction reactions is associated with the reversible hydride insertion step. It is interesting that no NaHFe(CO)₃L is observed. This could imply that HFe₂(CO)₇L has an unbridged hydride structure, with the hydride and PPh₃ ligands on different metal centers (e.g., (H)Fe–Fe(L)). Also worth noting is that, although the reaction NaHFe₂(CO)₈ + L to give NaHFe₂(CO)₇(L) + CO appears to occur for L = PPh₃, our data suggest that it is not important for L = RCH=CHCOR′.

NaHFe₂(CO)₈ Decomposition. NaHFe₂(CO)₈ was found to decompose by both acid-independent first-order as well as an acid-dependent second-order pathway, k_1 (total) = k_{1D} + k_{2D}[HOAc]. The NaHFe₂(CO)₈ decomposition mechanisms proposed, Scheme V, are consistent with the observed kinetics and stoichiometries. Thus, owing to these decomposition mechanisms, the disappearance of NaHFe₂(CO)₈ in reduction reactions is, in general, given by

$$-d[\text{NaHFe}_2(\text{CO})_8]/dt = \{2(k_{2R} + k_{3R}[\text{HOAc}]) + (k_{1D} + k_{2D}[\text{HOAc}])\}[\text{NaHFe}_2(\text{CO})_8]$$

However, for reactions with olefin in excess, the term k_{1D} + k_{2D}[HOAc] is negligible as shown by the zero intercept of Figure 8. It is interesting to note that the ratio of the rates of metal–metal bond cleavage to protonolysis (to give H₂) measured for NaHFe₂(CO)₈ decomposition, k_{1D}/k_{2D} = 0.09 M/[HOAc], are the same within experimental error as the ratio of metal–metal bond cleavage to protonolysis (to give RCH₂CH₂COR′) found in the reduction reactions, k_{2R}/k_{3R}[HOAc] = 0.1 M/[HOAc].

Summary and Conclusions

This study describes the use of NaHFe₂(CO)₈ for the reduction of activated olefins including detailed evidence for the mechanism of these reductions. The key pieces of evidence for this mechanism are (1) a first-order dependence upon NaHFe₂(CO)₈ and activated olefin, i.e., a bimolecular, associative first step; (2) a reversible, regiospecific hydride addition step; (3) a reasonably large, inverse deuterium isotope effect.

We speculate that the above pieces of evidence will serve as diagnostics of a hitherto little appreciated, yet general, mechanism of metal hydride reductions of activated olefins.

Also noteworthy from this study is the magnitude of effort

required to establish the reactive species in a cluster reaction—even for a binuclear cluster, the simplest of all clusters. Quite clearly distinguishing between catalysis by cluster fragments, catalysts by "heterogeneous" metal from cluster decomposition, and true intact cluster catalysis is an important and difficult problem. General methods for solution of the above problems are currently under investigation.

Experimental Section

A. General. 1. Methods for Handling Air-Sensitive Compounds. Air- and water-free conditions were maintained at all times throughout this work. A Vacuum Atmospheres Co. HE-193-1 recirculating inert atmosphere (nitrogen) drybox was used for the storage of Na₂Fe(CO)₄-1.5dioxane, Na₂Fe₂(CO)₈, all solvents, HOAc, and all materials used for kinetic determinations. The level of O₂ and other impurities (H₂O, R₃N, and ROH) was monitored with Et₂Zn which fumes at ≥5 ppm impurities, and with a light bulb with a hole in it, which generally burned for 2 or 3 weeks, indicating ≤1 ppm impurities. All flasks and vials used in the kinetic experiments were dried at 140 °C overnight, then held under vacuum followed by cooling under nitrogen. Liquid transfers outside the drybox were handled by syringe and needlestock techniques. Nitrogen (99.996%) was further purified by passage through a BASF oxygen scavenger and Linde 3A molecular sieve.

2. Materials. Tetrahydrofuran (THF) was doubly distilled under nitrogen, first from CaH₂ in a recirculating still, then from sodium/benzophenone into a dry, nitrogen-filled flask. reagent grade N-methylpyrrolidinone (NMP) was refluxed over CaH₂ at reduced pressure for at least 2 days, followed by distillation into a dry flask containing activated 3A or 13X molecular sieve, followed by distillation from these molecular sieves into a dry flask. 1,4-Dioxane was distilled from CaH₂ under nitrogen. THF-d_8 (Merck Sharp and Dohme, Canada, Ltd.), 99% d, was used without further purification.

With the following exceptions organic substrates were commercially available and were dried and distilled before use. Ethyl crotonate was dried with CaCl₂ and distilled using a spinning band column. 4,4-Dimethylcyclohexenone,[84] dihydrocarvone,[85] 6,6-dimethyl-2-cyclohexenone,[86] γ-crotonolactone,[87] and Δ[1,9]-2-octalone[88] were prepared using literature methods.

Na₂Fe(CO)₄-1.5dioxane was prepared by the method of Komoto.[89] Acetic acid was refluxed with acetic anhydride and chromium trioxide, followed by fractionation. DOAc (CD₃CO₂D) was purchased from Fisher Scientific, and used as received. Fe(CO)₅ (PCR, Inc.) was filtered, degassed, and stored over molecular sieve. Carbon monoxide (Liquid Carbonic, 99.5%) and ¹³C-labeled carbon monoxide (Monsanto Research Co.) were used without further purification. Triphenylphosphine was recrystallized from ethanol and dried in an Abderhalden. Bis(triphenylphosphine)iminium chloride (PPN⁺Cl⁻) was prepared by the method of Ruff,[23] recrystallized from water, and dried in an Abderhalden. Anhydrous lithium bromide was prepared from 1,2-dibromoethane and lithium.[90] Dicyclohexyl-18-crown-6 (Aldrich technical grade) was purified by chromatography on neutral alumina (eluting with an Et₂O–hexane mixture) to give the A and B isomers as a white, crystalline solid (mp 45–60 °C). Superior purification methods are now available.[91]

3. Equipment. Infrared spectra were obtained on a Perkin-Elmer 521 spectrophotometer. ¹H NMR spectra were obtained on a Varian A-60 spectrometer and 100-MHz ¹H and ¹³C NMR spectra were obtained on a Varian XL-100 spectrometer. GC–mass spectral data were obtained with a Varian 2100 gas chromatograph coupled to a Varian CH-7 mass spectrometer. Conductivity measurements were made using an Industrial Instruments Model RC 13B2 bridge with a Yellow Springs Model 3403 dip cell (cell constant = 1.0). Temperature control to ±0.1 °C was maintained with a Forma-Temp Jr. constant temperature bath, and was monitored using a 76-mm immersion thermometer calibrated from −1 to 101 °C by 0.1 °C (VWR Scientific Co., no. 61032). A Varian E-12 spectrometer was used for EPR studies. Reactions were monitored by GLC on a Hewlett-Packard Model 5750 gas chromatograph with flame ionization detector (columns A, B, and C) and a Hewlett-Packard 5750 gas chromatograph with thermal conductivity detector (columns D, E, and F). The following columns were used for GLC analysis: column A, 10% OV-101 on Supelcon AWDMCS 80/100 mesh, 11 ft × ¹/₈ in. stainless steel tubing; column B, 10% Carbowax 20M on Chromosorb

W AW, 80/100 mesh, 6.5 ft × ⅛ in. stainless steel tubing; column C, 30% saturated AgNO₃ in benzyl cyanide on Chromosorb P, 80/100 mesh, 5 ft × ⅛ in. stainless steel tubing; column D, 10% diethylene glycol adipate ester on Chromosorb A AW, 7 ft × ¼ in. glass column, used with glass injector and exit port; column E, 10% SE-30 on Chromosorb W, 80/100 mesh, 7 ft × ¼ in. aluminum tubing; column F, 15% MnCl₂ on Alcoa F1 alumina, 48/100 mesh, 12 ft × ¼ in. copper tubing, followed by a tubular (10 × ¾ in.) CuO furnace kept at 500 °C; column G, 3% OV-101 on Chromosorb Q, 100/120 mesh, 6 ft × ¼ in glass column.

B. Preparation of Na₂Fe₂(CO)₈. In a drybox 10 g (28.9 mmol) of Na₂Fe(CO)₄·1.5dioxane was added to a 500-mL round-bottom flask equipped with magnetic stir bar and side arm. To this was added 200 mL of THF, and the flask was sealed with a serum stopper and removed from the drybox. The flask was attached to a bubbler and 3.90 mL of Fe(CO)₅ (28.9 mmol) was added via syringe. The solution was vigorously stirred for 3 h, during which time vigorous CO evolution ensued (caution). The solution turned red and precipitated orange Na₂Fe₂(CO)₈·xTHF (x was shown to be between 3 and 4 by ¹H NMR analysis). Under positive nitrogen pressure, 200 mL of freshly distilled, degassed petroleum ether was added. The solution was decanted and washed twice more with petroleum ether. Residual solvent was removed in vacuo with a hot water bath, yielding a bright yellow powder. GLC analysis of the resulting Na₂Fe₂(CO)₈ in hexamethylphosphoramide showed only a trace of residual THF. Infrared bands were observed at 1914 (sh), 1868 (s), and 1821 cm⁻¹ (m) in THF. The Na₂Fe₂(CO)₈ was stored in a drybox.

C. Preparation of Homogeneous Solutions of M⁺HFe₂(CO)₈⁻. 1. M⁺ = Na⁺. Na₂Fe₂(CO)₈ (0.764 g, 2.00 mmol) was weighed into a 10.3 × 2.2 cm test tube equipped with magnetic stir bar. With a pipette, 20.0 mL of THF was added. Via syringe 0.112 mL of HOAc (2.00 mmol) was added, and the test tube was sealed with a serum stopper, removed from the drybox, and immediately placed in ice. The sample was centrifuged for 5–10 min. Samples prepared in this method yielded about 12–13 mL of yellow-brown, homogeneous 0.10 M NaHFe₂(CO)₈ solutions: νmax (THF) 1987 (s), 1940 (s), 1880 (s), 1852 (sh), 1770 (m), and 1730 cm⁻¹ (w); δ (THF, benzene 7.266 ppm) −8.47 (32 °C). Although NaHFe₂(CO)₈ decomposes slowly at ambient temperature, the solutions were stable for a few days in a −22 °C freezer, and were further manipulated in a drybox. These solutions were found to reduce excess dimethyl maleate with excess HOAc in 97% yield based on iron in 13 min (after 24 h, greater than 100% yields can be obtained).

2. M⁺ = PPN⁺. To 15 mL of 0.10 M homogeneous NaHFe₂(CO)₈ was added 0.861 g of PPNCl (1.52 mmol) in a centrifuge tube. The tube was sealed with a serum stopper, shaken, cooled in ice, and centrifuged to yield a homogeneous, yellow-brown solution of 0.1 M (PPN)⁺(HFe₂(CO)₈)⁻: νmax (THF) same as sodium salt except that 1730-cm⁻¹ band was completely absent.

3. M⁺ = Li⁺. To 25 mL of homogeneous 0.10 M NaHFe₂(CO)₈ in THF was added 0.218 g of LiBr (2.5 mmol). The solution was shaken and centrifuged as previously described to give a 0.10 M homogeneous solution of LiHFe₂(CO)₈: νmax (THF) same as that of sodium salt except that the 1730-cm⁻¹ absorbance has been replaced by an absorbance at 1618 cm⁻¹.

4. M⁺ = crown·Na⁺. To 20 mL of homogeneous 0.10 M NaHFe₂(CO)₈ in THF was added 0.745 g of dicyclohexyl-18-crown-6 (2.0 mmol). The solution was stirred and used without further purification to give a homogeneous 0.10 M solution of crown·Na⁺HFe₂(CO)₈⁻: νmax (THF) same as that of sodium salt except that the 1730-cm⁻¹ absorbance was completely absent; δ (THF, benzene 7.266) −9.01 (32 °C).

D. Preparation of Homogeneous Solutions of NaHFe(CO)₄. Pale yellow, homogeneous THF solutions (up to 0.3 M) of NaHFe(CO)₄ were prepared from Na₂Fe(CO)₄·1.5dioxane and HOAc using the method described to prepare homogeneous NaHFe₂(CO)₈ solutions: νmax (THF) 1997 (m), 1903 (sh), 1878 (s), 1851 cm⁻¹ (sh); δ (THF, benzene 7.266) 8.74 at 32 °C.

E. Synthetic Reduction Procedures Using NaHFe₂(CO)₈ and HOAc in THF. 1. Reduction of d-Carvone. Using the procedure previously described, 11.5 mmol of Na₂Fe₂(CO)₈·x THF was prepared in 75 mL of THF. To this was added HOAc (1.0 mL, 18 mmol) followed by 0.94 mL of d-carvone (6 mmol). After sitting for 12 h, the resulting purple solution was poured into 100 g of ice, followed by addition of 75 mL of Et₂O. With stirring, FeCl₃ was added (caution: CO evolution) until further addition of FeCl₃ yielded little gas evolution. The green ether

solution was extracted with dilute HCl, water, saturated NaHCO₃, water, and saturated NaCl and then dried with MgSO₄. After concentration on a spinning evaporator, the resulting oil was eluted with heptane on a 4.5 × 10 cm silica gel column until all the green Fe₃(CO)₁₂ was removed. The product was eluted with diethyl ether and concentrated on a spinning evaporator. Bulb-to-bulb distillation gave 0.69 g of crude product. GLC analysis on both column A (157 °C) and column B (210 °C) showed two components, one that coinjected with d-carvone and one that coinjected with authentic dihydrocarvone. Dihydrocarvone accounted for 46% of the crude product (35% total yield). A small sample of dihydrocarvone was isolated by preparative GLC: νmax (neat) 3080, 1713, 1645, 888 cm⁻¹ (lit.[85] 3100, 1710, 1650, 892 cm⁻¹); δ (CDCl₃) 1.00 and 1.08 (3 H, two doublets, relative area 3.3/1, J = 6.0 and 6.5 Hz, respectively, for the epimeric trans-1,4 and cis-1,4 CHMe, respectively), 1.72 (3 H, MeC=CH₂), and 4.69 (2 H, MeC=CH₂).

2. Reduction of Acylamide. To a suspension of 10 mmol of Na₂Fe₂(CO)₈ in 75 mL of THF prepared as described was added 1.14 mL of HOAc (20 mmol) and 0.36 g of acrylamide (5 mmol). After 15 h, the solution was worked up as described except that Cu(OAc)₂ was used to oxidize the residual iron hydrides, to yield 185 mg (50%) of propionamide: νmax (THF) 1680 cm⁻¹; δ (CDCl₃) 1.15 (3 H, triplet, J = 7.4 Hz), 2.17 (2 H, quartet, J = 7.4 Hz), 6.5 (2 H, broad singlet).

3. Reduction of Cinnamonitrile. To a suspension of 20 mmol of Na₂Fe₂(CO)₈ in 100 mL of THF was added 1.14 mL of HOAc (20 mmol) and 1.25 mL of cinnamonitrile (10 mmol). After stirring overnight the iron carbonyl by-products were oxidized with Ce(NO₃)₆(NH₄)₂ and diethyl ether and dilute HCl were added. The ether layer was successively extracted with HCl, dilute NaHCO₃, and brine. The solution was dried with MgSO₄ and the solvent removed on a spinning evaporator. This gave 1.47 g of crude product which was found to be 83% pure by GLC (column A, 200 °C) for an isolated yield of 93%. A small sample was purified by distillation on a micro-spinning band column to give pure hydrocinnamonitrile: νmax (neat) 3035, 2235, 1496, 1403, 746, 696 cm⁻¹; δ (CCl₄) 2.40, 2.51, 2.70, 2.79 (4 H, major peaks in multiplet), 7.16 (5 H, phenyl protons).

4. Reduction of γ-Crotonolactone. Using 12 mmol of Na₂Fe₂(CO)₈ and 18 mmol of HOAc in 75 mL of THF, 0.50 g of γ-crotonolactone (6 mmol) was reduced in the usual fashion to yield 0.39 g of γ-butyrolactone (76%): δ (CDCl₃) 4.33 (2 H, triplet, J = 6.1 Hz), 2.35, 2.41, 2.47 (4 H, major peaks in multiplet).

5. Reductions without Isolation. Yields in Table I were determined by GLC using internal standards and were corrected for molar responses. Products were identified by coinjection of authentic materials. Generally, 1–2 mmol of Na₂Fe₂(CO)₈ was generated in situ in 10 mL of THF. The amount of substrate and acid added is given in Table I.

F. Synthetic Reduction Procedures Using Na₂Fe(CO)₄–1.5Dioxane, Fe(CO)₅, and HOAc in 1,4-Dioxane. 1. Reduction of Δ¹,⁹-2-Octalone. In an inert atmosphere box, 2.08 g of Na₂Fe(CO)₄·1.5dioxane (6.0 mmol) was added to 50 mL of 1,4-dioxane in a 125-mL Erlenmeyer flask equipped with magnetic stir bar. The flask was sealed with a serum stopper and removed from the inert atmosphere box. Via syringe, 0.810 mL of Fe(CO)₅ (6 mmol), 0.684 mL of HOAc (12.2 mmol), and 0.166 g of Δ¹,⁹-2-octalone (1.0 mmol) were added. The solution was stirred overnight. The purple iron by-products were decomposed with Clorox (caution: CO evolution). The organic products were extracted with diethyl ether, dried with magnesium sulfate, and concentrated on a spinning evaporator. Separation from the residual iron by-products was achieved by elution on a 20 × 20 × 0.1 cm preparative TLC plate with 8:1 hexane/diethyl ether to give 0.140 mg of 2-decalone (91%). GLC analysis[62a] (column E, 220 °C) showed cis:trans, 87:13. The cis peak was coinjected with authentic cis-2-decalone.

2. Reductions without Isolation. Yields in Table II were determined by GLC using internal standard and were corrected for molar responses. Products were identified by coinjection of authentic materials. Generally, 1–2 mmol of Na₂Fe(CO)₄–1.5dioxane in 10 mL of dioxane was used. The amount of Fe(CO)₅, acid, and substrate is given in Table II.

G. Kinetic Procedures. 1. GLC Kinetics. Substrate Reduction. The kinetic procedure for the reduction of trans-ethyl crotonate with NaHFe₂(CO)₈ and HOAc will be presented as a typical example. In the drybox, 20.0 mL of homogeneous 0.10 M NaHFe₂(CO)₈ containing 0.0056 M nonane was transferred to a 25-mL Erlenmeyer flask

which was subsequently sealed with a serum stopper and thermostated to 25.0 °C. Via tubing attached to a syringe needle, the flask was attached to a nitrogen bubbler and kept under a slight positive nitrogen pressure. The kinetic run was initiated by simultaneous injection of 0.025 mL of ethyl crotonate (0.010 M) and 0.100 mL of HOAc (0.098 M) and vigorous swirling. Nine 0.20-mL aliquots, covering 0–90% reaction, were removed and quenched by injecting them, via gas-tight syringe, into N$_2$-filled, serum-stoppered vials containing 0.010 mL of dimethyl maleate (0.40 M) and 0.005 mL of HOAc (0.53 M). The samples were simultaneously analyzed for product, reactant, and nonane internal standard by flame ionization GLC (column A, 90 °C), giving two values for the rate constant for each run. Quantification was generally accomplished using peak heights, although identical results were obtained using a Vidar 6300 digital integrator or cut and weigh analysis. These GLC rate constants are precise to ±15%.

2. IR Kinetics. Substitution of NaHFe$_2$(CO)$_8$ with PPh$_3$. To determine [NaHFe$_2$(CO)$_8$] at time = 0, the absorbance of the 1770-cm^{-1} band of a 0.080 M homogeneous NaHFe$_2$(CO)$_8$ solution in THF was measured using solution IR cells equipped with CaF$_2$ windows separated by 0.1-mm amalgamated lead spacers. The reaction was initiated by injection with a gas-tight syringe of 10.0 mL of the NaHFe$_2$(CO)$_8$ solution onto 1.048 g of PPh$_3$ (4.0 mmol) in a N$_2$-filled serum stopper Erlenmeyer thermostated to 25.0 °C, followed by agitation to ensure mixing. The concentration of NaHFe$_2$(CO)$_8$ was determined from the absorbance of the 1770-cm^{-1} peak. This was done by injecting aliquots of the reaction solutions into the N$_2$-purged, serum-stoppered, clean IR cells. The time was recorded as the 1770-cm^{-1} peak was traced. Nine kinetic points were determined in this manner, over 82% reaction.

3. ^{1}H NMR Kinetics. (a) Decomposition of NaHFe$_2$(CO)$_8$. A typical procedure to measure the rate of decomposition is as follows. To determine [NaHFe$_2$(CO)$_8$] at time = 0, 0.5 mL of a homogeneous 0.10 M NaHFe$_2$(CO)$_8$ solution containing 0.019 M benzene was placed in a sealed NMR tube. The decomposition was initiated by addition of 0.125 mL of HOAc (0.436 M) to 5.0 mL of the remaining NaHFe$_2$(CO)$_8$ solution. The concentration of NaHFe$_2$(CO)$_8$ was measured at various times by ^{1}H NMR by comparing the peak heights of the NaHFe$_2$(CO)$_8$ and the benzene standard. Both the hydride and benzene peak heights were measured three times per kinetic point. Between ^{1}H NMR measurements, the ^{1}H NMR tube was stored at 25.0 °C. Eight kinetic points were measured and the decomposition was followed to 77% completion.

(b) Rate of Ethyl Crotonate Reduction. Using the techniques described, 0.295 mL of 0.20 ± 0.02 M homogeneous NaHFe$_2$(CO)$_8$ containing 0.028 M benzene was prepared in THF-d_8 and transferred to a ^{1}H NMR tube. After sealing with a serum stopper and equilibrating in the probe (at 25 ± 1 °C) of a Varian XL-100 NMR spectrometer, the reduction was initiated by injecting 0.0020 mL of HOAc (0.12 M) and 0.0073 mL of ethyl crotonate (0.20 M) and shaking. The concentration of product and reactant was determined by comparing the peak height of the benzene standard with the peak height of the center triplet at 0.87 ppm (ethyl butyrate) and the doublet at 1.83 ppm (ethyl crotonate). Eight kinetic points were determined in this manner over 82% reaction.

(c) Rate of Cleavage of (PPN)$^+$[CH$_3$CH(Fe(CO)$_4$)CO$_2$Et]$^-$ with HOAc. The rate of cleavage of (PPN)$^+$[CH$_3$CH(Fe(CO)$_4$)CO$_2$Et]$^-$ with HOAc to form ethyl propionate was monitored by ^{1}H NMR using a 0.125 M solution of the complex in THF-d_8, prepared from 0.040 g of isolated (PPN)$^+$[CH$_3$CH(Fe(CO)$_4$CO$_2$Et]$^-$ and 0.40 mL of THF-d_8. After equilibration of the sample to 35 °C in the ^{1}H NMR probe, the concentration of the complex at time = 0 was measured. The reaction was initiated by injection of 0.0050 mL of HOAc (0.22 M). The concentration of iron complex was determined by comparison of the peak height of the doublet (δ 1.5) due to the complex with the peak height of the residual THF-d_8 singlet (δ 1.8). Six kinetic points were measured and the reaction was followed to 56% completion.

4. Experiments under Constant CO Pressure. CO Uptake. A hydrogenation apparatus modeled after the constant-pressure apparatus developed by Madon[92] was filled with CO at 1 atm. To the water-jacketed reaction vessel, thermostated to 25.0 °C, was added 0.050 mL (0.88 mmol) of HOAc followed by 10 mL of 0.10 M homogeneous NaHFe$_2$(CO)$_8$ in THF. The solution was stirred rapidly to ensure proper mixing and the CO uptake at 1 atm pressure was measured as a function of time. The same apparatus was used to determine the CO dependence of the reduction of ethyl crotonate.

5. Analysis of Kinetic Data. Rate constants for kinetic data, obtained

under pseudo-first-order conditions, were found by least-squares fit using two basic equations, one for the loss of reactant and one for the formation of product, where

$$\ln R_0/R_t = k_1 t$$

$$\ln P_\infty/(P_\infty - P_t) = k_1 t$$

R_0 = reactant concentration at time = 0, R_t = reactant concentration at time = t, P_∞ = product concentration at >10 half-lives, and P_t = product concentration at time = t. Data for the rate of NaHFe$_2$(CO)$_8$ decomposition (^{1}H NMR kinetics) and substrate reduction (GLC kinetics) were treated in this way. For kinetic data obtained for substitution of NaHFe$_2$(CO)$_8$ by PPh$_3$ (IR kinetics) and substrate reduction (^{1}H NMR kinetics), rate constants were determined by plotting concentration of reactant or product vs. time, measuring the initial rate for loss of reactant or formation of product, and dividing the initial rate by the initial concentrations. Further details on the treatment of kinetic data can be found in the text.

H. Stoichiometry. 1. Reduction in the Absence of Acid. A homogeneous 0.01 M NaHFe$_2$(CO)$_8$ in THF was prepared containing 0.014 M benzene, 0.077 M hexane, and 0.028 M nonane. To 4 mL of this solution was added 0.200 mL of ethyl crotonate (0.40 M), the reaction flask was covered with aluminum foil (to prevent Fe(CO)$_5$ + $h\nu$ → Fe$_2$(CO)$_9$) and allowed to stand overnight. The following components were analyzed.

(a) Fe(CO)$_5$: GLC (column D, 40 °C) showed 0.028 ± 0.004 M Fe(CO)$_5$ using hexane as an internal standard and correcting for molar responses.

(b) NaHFe$_2$(CO)$_8$: ^{1}H NMR analysis showed no NaHFe$_2$(CO)$_8$ (δ 8.47).

(c) NaHFe(CO)$_4$: ^{1}H NMR analysis showed no NaHFe(CO)$_4$ (δ 8.74).

(d) NaHFe$_3$(CO)$_{11}$: ^{1}H NMR analysis showed 0.024 ± 0.003 M NaHFe$_3$(CO)$_{11}$ (δ 14.87) by comparing the peak heights for benzene and the hydride. The hydride peak was multiplied by a 1.14 correction factor, which was determined independently from a known solution of [Et$_3$NH][HFe$_3$(CO)$_{11}$], THF, and benzene. After acid quench, the amount of NaHFe$_3$(CO)$_{11}$ rose to 0.035 ± 0.005 M.

(e) Fe$_3$(CO)$_{12}$: a sample of solution was examined by visible spectroscopy for an absorption at 6050 Å. None was found.

(f) Organic products: the sample was quenched with 0.080 mL of HOAc (0.45 M) and 0.080 mL of dimethyl maleate (0.14 M) and analyzed by GLC (column A, 90 °C), correcting for molar responses. Comparison of the peak heights of the nonane standard with the organic products showed 0.057 M ethyl butyrate, 0.032 M cis-ethyl crotonate, and 0.271 M trans-ethyl crotonate.

(g) Na$_2$Fe$_3$(CO)$_{11}$: in a separate experiment, 20 mL of 0.10 M NaHFe$_2$(CO)$_8$ was treated with 0.180 mL of methyl acrylate (0.20 M). After 5.5 h, 1.148 g of PPN$^+$Cl$^-$ (2.0 mmol) was added. The THF was removed in vacuo, 10 mL of acetone was added, and the solution was filtered. Addition of 7 mL of diethyl ether resulted in the formation of deep red crystals identified as (PPN)$_2$(Fe$_3$(CO)$_{11}$), 5% yield: ν_{max} (KBr) 1933 (s), 1897 (s), 1883 cm^{-1} (sh) (lit.[93] (DMF) 1941 (s), 1913 (m), 1884 cm^{-1} (w)).

Anal. Calcd for C$_{83}$Fe$_3$H$_{60}$N$_2$O$_{11}$P$_4$: C, 64.20, H. 3.88; N. 1.80. Found: C, 63.79; H, 3.97; N, 1.72.

2. PPh$_3$ Substitution of NaHFe$_2$(CO)$_8$. To 0.300 g of PPh$_3$ (1.15 mmol) was added 5.0 mL of homogeneous 0.10 M NaHFe$_2$(CO)$_8$ in THF, which contained 0.014 M benzene and 0.077 M hexane. After 12 h, the following components were analyzed.

(a) Fe(CO)$_5$: 0.04 ± 0.01 M by GLC as described.

(b) Fe(CO)$_4$L: an aliquot was injected into nitrogen-purged serum stoppered solution IR cells (CaF$_2$, 0.1 mm amalgamated lead spaces) and the absorbance of the 2055-cm^{-1} band due to Fe(CO)$_4$PPh$_3$ was measured (ϵ 2200 L mol^{-1} cm^{-1}, measured independently). Although Fe(CO)$_5$ interfered with this determination, the amount of Fe(CO)$_4$L was found to be 0.022 ± 0.006 M.

(c) NaHFe(CO)$_4$: ^{1}H NMR analysis showed NaHFe(CO)$_4$ (δ 8.74) to be the only iron hydride present. The amount of NaHFe(CO)$_4$ could not be quantified with the benzene standard owing to the triphenylphosphine phenyl protons. In a separate experiment with methylcyclohexane used as a standard, the amount of NaHFe(CO)$_4$ was found to be 0.10 ± 0.05 M.

(d) NaHFe(CO)$_3$PPh$_3$: in a separate experiment, the substitution of 0.2 M NaHFe$_2$(CO)$_8$ by 0.4 M PPh$_3$ was monitored by ^{1}H NMR (methylcyclohexane standard). The singlet due to NaHFe$_2$(CO)$_8$ (δ

8.47) was found to decrease smoothly as the singlet due to NaH-Fe(CO)$_4$ (δ 8.74) grew in. At no time was the doublet (δ 9.39, $J = 43$ Hz) due to NaHFe(CO)$_3$L observed.

(e) Fe(CO)$_3$L$_2$: filtration of the solution gave 0.121 g of Fe-(CO)$_3$(PPh$_3$)$_2$ (0.18 mmol, which corresponds to 0.038 M), ν_{max} (KBr) 1870 cm^{-1} (lit.[94] 1884.8 cm^{-1}).

Anal. Calcd for C$_{57}$FeH$_{45}$O$_3$P$_3$: C, 69.38; Fe, 8.06; H, 4.33; P, 8.96. Found: C, 70.12; Fe, 8.11; H, 4.62; P, 8.70.

I. Substitution of NaHFe(CO)$_4$ with PPh$_3$. 1. No HOAc. The hydride resonance of 0.50 mL of homogeneous 0.10 M NaHFe(CO)$_4$ solution containing 0.20 M PPh$_3$ and 0.45 M benzene was monitored by ^{1}H NMR. No change was observed over 3 h.

2. With HOAc. To the above solution was added 0.010 mL of HOAc (0.35 M). The singlet due to NaHFe(CO)$_4$ decreased and a doublet (δ 9.39, $J = 43$ Hz) grew in (due to NaHFe(CO)$_3$L formation) which reached a maximum within 4 min. Subsequently, this doublet decreased with time and was virtually gone in 15 min. Hydrogen was identified above a similar solution by GLC (column F, -198 °C).

J. Preparation of Na[CH$_3$CH$_2$CH(Fe(CO)$_4$)CO$_2$Et]. To 4.0 mL of homogeneous 0.20 M NaHFe(CO)$_4$ in THF was added 0.124 mL of ethyl crotonate (0.25 M). Heating for 12 h in a 40 °C oil bath yielded a homogeneous orange solution of Na[CH$_3$CH$_2$CH(Fe(CO)$_4$)-CO$_2$Et]: ν_{max} (THF) 1665 cm^{-1}; NMR and ^{13}C NMR data as presented in Tables III and IV.

K. ^{13}CO Exchange with NaHFe$_2$(CO)$_8$ and NaHFe(CO)$_4$. To each of three ^{13}C NMR tubes were added 2.5 mL of homogeneous 0.20 M NaHFe$_2$(CO)$_8$, 0.500 mL of benzene-d_6, and 0.100 mL of Me$_4$Si. Two other ^{13}C NMR tubes were similarly prepared with 0.20 M NaHFe(CO)$_4$. One sample each of NaHFe$_2$(CO)$_8$ and NaHFe(CO)$_4$ were used as blanks, and one sample each was thermostated to 25.0 °C and bubbled with 20% ^{13}CO for 3.0 min followed by N$_2$ for 3.0 min. Immediately before bubbling, 0.062 mL of ethyl crotonate (0.50 mmol) was added to the third sample of NaHFe$_2$(CO)$_8$. The flow rates for ^{13}CO and N$_2$ were kept constant for all samples, and the samples were stored in a dry ice bath between manipulations. ^{13}C NMR data was collected in an identical manner for each, using 4K transients (acquisition time 0.533 s, flip angle about 55°) over a spectrum width of 7500 Hz to give a data table and Fourier transform length of 8192. Probe temperature was kept at -40 to -50 °C. The resulting spectra were plotted in the absolute intensity mode (Hz/point $= 1.88$). The height of the M $-$ CO absorbance was maximized before plotting.

L. Olefin Cis/Trans Isomerization. To 5.0 mL of homogeneous 0.10 M NaHFe$_2$(CO)$_8$ was added 0.064 mL of cis-3-hexene. The amounts of cis- and trans-3-hexene were analyzed at various times by GLC (column C, 25 °C).

M. Equivalent Conductance vs. Dilution. Six serial dilutions of an originally 0.10 M NaHFe$_2$(CO)$_8$ solution in THF were made in the drybox, yielding the most dilute solution at $(0.10/64) = 1.56 \times 10^{-3}$ M. Starting with the most dilute solution, the conductance at each dilution was measured.

N. Deuterium Labeling Studies. Samples for GC–mass spectral analysis were prepared by reducing 0.05 M solutions of substrate with homogeneous 0.20 M NaDFe$_2$(CO)$_8$ and 0.10 M CD$_3$CO$_2$D. Aliquots were quenched at appropriate times using dimethyl maleate and CD$_3$CO$_2$D as described for GLC kinetics. Samples were separated by GC (column G) and analyzed by their mass spectra (source voltage, 20 eV; source temperature, 175 °C; filament current, 100 μA).

O. Reaction of Fe(CO)$_4$(ethyl cinnamate) with NaHFe(CO)$_4$ and HOAc. To a solution of 0.1 M NaHFe(CO)$_4$ and 0.1 M HOAc was added 1 mmol of Fe(CO)$_4$(ethyl cinnamate). The solution rapidly discolored. No high initial yield of ethyl dihydrocinnamate was observed. Instead, ethyl dihydrocinnamate was formed in about the same yield and rate as was formed from 0.1 M NaHFe$_2$(CO)$_8$, 0.1 M HOAc, and 0.1 M ethyl cinnamate.

P. Reaction of NaHFe(CO)$_4$, Fe(CO)$_4$(PPh$_3$), and PPh$_3$. A THF solution containing 0.20 M NaHFe(CO)$_4$, 0.20 M Fe(CO)$_4$(PPh$_3$), 0.20 M PPh$_3$, and 0.12 M Me$_4$Si was examined by ^{1}H NMR over the course of 4 h. No changes in intensity or position of the NaHFe(CO)$_4$ resonance or the resonances due to the phenyl protons in the Fe(CO)$_4$PPh$_3$ and the PPh$_3$ were observed. The solution remained pale yellow throughout.

References and Notes

(1) For reviews of transition metal carbonyl clusters see (a) R. B. King, *Prog. Inorg. Chem.*, **15**, 287 (1972); (b) P. Chini, *Inorg. Chim. Acta Rev.*, **2**, 31 (1968); (c) E. W. Abel and F. G. A. Stone, *Q. Rev., Chem. Soc.*, **23**, 325 (1969); (d) M. C. Baird, *Prog. Inorg. Chem.*, **9**, 1 (1968); (e) R. D. Johnston, *Adv. Inorg. Chem. Radiochem.*, **13**, 471 (1970); (f) S. C. Tripathi, S. C. Srivastava, R. P. Mani, and A. K. Shrimal, *Inorg. Chim. Acta Rev.*, **17**, 257 (1976); (g) F. A. Cotton, *Q. Rev., Chem. Soc.*, **20**, 389 (1966); (h) P. Chini, G. Longoni, and V. G. Albano, *Adv. Organomet. Chem.*, **14**, 285 (1976); (i) P. Chini, *Pure Appl. Chem.*, **23**, 489 (1970); (j) B. P. Biryukov and Yu. T. Struchkov, *Russ. Chem. Rev. (Engl. Transl.)*, **39**, 789 (1970).

(2) (a) E. L. Muetterties, "Transition Metal Hydrides", Marcel Dekker, New York, N.Y., 1971; (b) H. D. Kaesz and R. B. Saillant, *Chem. Rev.*, **72**, 231 (1972); (c) H. D. Kaesz, *Chem. Br.*, **9**, 344 (1973); (d) J. P. McCue, *Coord. Chem. Rev.*, **10**, 265 (1973).

(3) K. Wade, *Chem. Br.*, **11**, 177 (1975), and references cited therein; *Adv. Inorg. Chem. Radiochem.*, **18**, 1 (1976); R. N. Grimes, *Ann. N.Y. Acad. Sci.*, **239**, 180 (1974); R. W. Rudolph. *Acc. Chem. Res.*, **9**, 446 (1976).

(4) Recent reports of new clusters include (see also ref 5b–e) (a) G. Longoni, P. Chini, L. D. Lower, and L. F. Dahl, *J. Am. Chem. Soc.*, **97**, 5034 (1975); (b) J. C. Calabrese, L. F. Dahl, A. Cavalieri, P. Chini, G. Longoni, and S. Martinengo, *Ibid.*, **96**, 2616 (1974); (c) J. C. Calabrese, L. F. Dahl, P. Chini, G. Longoni, and S. Martinengo, *Ibid.*, **96**, 2614 (1974); (d) R. S. Gall, N. G. Connelly, and L. F. Dahl, *ibid.*, **96**, 4017 (1974); (e) R. C. Ryan and L. F. Dahl *ibid.*, **97**, 6904 (1975); (f) O. M. Abu Salah and M. I. Bruce, *J. Chem. Soc., Chem. Commun.*, 858 (1972); (g) R. J. Klingler, W. Butler, and M. D. Curtis, *J. Am. Chem. Soc.*, **97**, 3535 (1975); (h) J. G. Albano, A. Ceriotti, P. Chini, G. Ciani, S. Martinengo, and W. M. Anker, *J. Chem. Soc., Chem. Commun.*, 859 (1975); (i) C. R. Eady, B. F. G. Johnson, J. Lewis, B. E. Reichert, and G. M. Sheldrick, *ibid.*, 271 (1976); (j) J. L. Davidson, M. Green, F. G. A. Stone, and A. J. Welch, *J. Am. Chem. Soc.*, **97**, 7490 (1975); (k) V. W. Day, R. O. Day, J. S. Kristoff, F. J. Hirsekorn, and E. L. Muetterties, *Ibid.*, **97**, 2571 (1975); (l) J. R. Shapley, J. B. Keister, M. R. Churchill, and B. G. DeBoer, *ibid.*, **97**, 4145 (1975); (m) M. I. Bruce, G. Shaw, and F. G. A. Stone, *J. Chem. Soc., Chem. Commun.*, 1288 (1971); (n) *J. Chem. Soc., Dalton Trans.*, 1082 (1972).

(5) (a) L. M. Jackman and F. A. Cotton, "Dynamic Nuclear Magnetic Resonance Spectroscopy", Academic Press, New York, N.Y., 1975, Chapter 12; (b) Other recent studies of the fluxionality of metal carbonyl clusters include A. Forster, B. F. G. Johnson, J. Lewis, T. W. Matheson, B. H. Robinson, and W. G. Jackson, *J. Chem. Soc., Chem. Commun.*, 1042 (1974); (c) J. Lewis, B. F. G. Johnson, C. R. Eady, W. G. Jackson, and T. W. Matheson, *ibid.*, 958 (1975); (d) L. M. Lone, S. Aime, E. W. Randall, and E. Rosenberg, *ibid.*, 452 (1975); (e) C. R. Eady, B. F. G. Johnson, and J. Lewis, *ibid.*, 302 (1976); (f) F. A. Cotton and J. D. Jamerson, *J. Am. Chem. Soc.*, **98**, 1273 (1976).

(6) The situation in 1966 according to Cotton[1g] is only slightly improved today. "There does not yet appear to be any instance in which a synthetic reaction (or series of reactions) was deliberately designed to produce a particular cluster compound from mononuclear starting materials. On the contrary, all known clusters were discovered by chance or prepared unwittingly. Thus the student of cluster chemistry is in somewhat the position of the collector of lepidoptera or meteorites, skipping observantly over the countryside and exclaiming with delight when fortunate enough to encounter a new specimen."

(7) The chemical reactivity of H$_2$Os$_3$(CO)$_{10}$ has received considerable attention recently: (a) J. B. Keister and J. R. Shapely, *J. Am. Chem. Soc.*, **98**, 1056 (1976); (b) M. Tachikawa, J. R. Shapely, and C. G. Pierpont, *ibid.*, **97**, 7172 (1975), and references cited therein; (c) M. R. Churchill, B. G. DeBoer, J. R. Shapely, and J. B. Keister, *ibid.*, **98**, 2357 (1976); (d) A. J. Deeming, S. Hasso, and M. Underhill, *J. Chem. Soc., Dalton Trans.*, 1614 (1975); (e) J. B. Keister and J. R. Shapely, *J. Organomet. Chem.*, **85**, C29 (1975), and references cited therein; (f) A. J. Deeming and S. Hasso, *ibid.*, **88**, C21 (1975); (g) W. G. Jackson, B. F. G. Johnson, J. W. Kelland, J. Lewis, and K. T. Schorpp, *ibid.*, **87**, C27 (1975); (h) W. G. Jackson, B. F. G. Johnson, J. W. Kelland, J. Lewis, and K. T. Schorpp, *ibid.*, **88**, C17 (1975); (i) E. G. Bryan, B. F. G. Johnson, J. W. Kelland, and J. Lewis, *J. Chem. Soc., Chem. Commun.*, 254 (1976).

(8) For recent studies of the chemistry of Os$_3$(CO)$_{12}$ see (a) G. Gervasio, *J. Chem. Soc., Chem. Commun.*, 25 (1976); (b) M. G. Thomas, B. F. Beier, and E. L. Muetterties, *J. Am. Chem. Soc.*, **98**, 1296 (1976); (c) C. W. Bradford and R. S. Nyholm, *J. Chem. Soc., Dalton Trans.*, 529 (1973); (d) A. J. Deeming and M. Underhill, *J. Organomet. Chem.*, **42**, C60 (1972); (e) A. J. Deeming and M. Underhill, *J. Chem. Soc., Chem. Commun.*, 277 (1973).

(9) Other cluster reactions include (a) the reactions of a molybdenum–molybdenum triple bond: R. J. Klinger, W. Butler, and M. D. Curtis, *J. Am. Chem. Soc.*, **97**, 3535 (1975). (b) The reaction of Ru$_3$(CO)$_{12}$ and cyclo-hexa-1,3-diene: T. H. Whitesides and R. A. Budnik, *J. Chem. Soc., Chem. Commun.*, 87 (1973). (c) The oxidation of ketones using "Rh$_6$(CO)$_{16}$": G. D. Mercer, J. S. Shu, T. B. Rauchfuss, and D. M. Roundhill, *J. Am. Chem. Soc.*, **97**, 1967 (1975). (d) The reduction of α,β-unsaturated carbonyl and nitrile compounds using CO, H$_2$O, and Rh$_6$(CO)$_{16}$: T. Kitamura, N. Sakamoto, and T. Joh, *Chem. Lett.*, 379 (1973). (e) See also the articles cited in footnotes 90, 91, and 93 of ref 11.

(10) For mechanistic studies of the ligand substitution reactions involving carbonyl clusters see (a) K. J. Karel and J. R. Norton, *J. Am. Chem. Soc.*, **96**, 6812 (1974); (b) D. DeWitt, J. P. Fawcett, A. J. Poë, and M. V. Twigg, *Coord. Chem. Rev.*, **8**, 81 (1972), and references cited therein; (c) A. Poë and M. V. Twigg, *J. Chem. Soc., Dalton Trans.*, 1860 (1974), and references cited therein; (d) J. P. Fawcett, A. J. Poe, and M. V. Twigg, *J. Chem. Soc., Chem.*

Commun., 267 (1973); (e) J. P. Fawcett, R. A. Jackson, and A. Poe, *ibid.*, 733 (1975).

(11) E. L. Muetterties, *Bull. Soc. Chim. Belg.*, **84**, 959 (1975).

(12) G. Henrici-Olivé and S. Olivé, *Angew. Chem., Int. Ed. Engl.*, **15**, 136 (1976); H. H. Storch, N. Golumbic, and R. B. Anderson, "The Fischer-Tropsch and Related Syntheses", Wiley, New York, N.Y., 1951.

(13) M. Ichikawa, *J. Chem. Soc., Chem. Commun.*, 11 (1976); J. R. Anderson, R. J. Macdonald, and Y. Shimoyama, *J. Catal.*, **20**, 147 (1971).

(14) J. M. Dartigues, A. Chambellan, and F. G. Gault, *J. Am. Chem. Soc.*, **98**, 856 (1976).

(15) M. Boudart, "Effects of Surface Structure on Catalytic Reactivity", a preprint.

(16) T. J. Meyer, *Prog. Inorg. Chem.*, **19**, 1 (1975). However, problems resulting from weak metal–metal bonds may be minimized by the use of third-row transition metals.

(17) D. L. Morse and M. S. Wrighton, *J. Am. Chem. Soc.*, **98**, 3931 (1976), and references cited therein; D. S. Ginley and M. S. Wrighton, *ibid.*, **97**, 4908 (1975); M. S. Wrighton, *Top. Curr. Chem.*, **65**, 37 (1976).

(18) (a) E. L. Muetterties, B. A. Sosinsky, and K. I. Zamaraev, *J. Am. Chem. Soc.*, **97**, 5299 (1975); (b) J. P. Fawcett, R. A. Jackson, and A. Poë, *J. Chem. Soc., Chem. Commun.*, 733 (1975).

(19) There are two reports[8b,20] of what *appear* to be cluster catalysis of the Fischer–Tropsch reaction. However, the actual catalytically active species in these reports is still uncertain.

(20) *Chemtech*, 732 (1976), and references cited therein.

(21) (a) J. P. Collman, R. G. Finke, P. L. Matlock, and J. I. Brauman, *J. Am. Chem. Soc.*, **98**, 4685 (1976); (b) J. P. Collman, *Acc. Chem. Res.*, **8**, 342 (1975).

(22) Commercially available from Alfa-Ventron Corp.

(23) PPN⁺ = bis(triphenylphosphine)iminium cation. J. K. Ruff, *Inorg. Chem.*, **7**, 1818 (1968); J. K. Ruff and W. J. Schlientz, *Inorg. Synth.*, **15**, 84 (1974).

(24) H. B. Chin, Ph.D. Thesis, University of Southern California, Los Angeles, Calif., 1975.

(25) H. B. Chin, M. B. Smith, R. D. Wilson, and R. Bau, *J. Am. Chem. Soc.*, **96**, 5285 (1974).

(26) H. M. Powell and R. V. G. Ewens, *J. Chem. Soc.*, 286 (1939).

(27) R. M. Fuoss and F. Accascina, "Electrolytic Conductance", Interscience, New York, N.Y., 1959, Chapter 18.

(28) J. P. Collman, R. G. Finke, P. L. Matlock, and J. I. Brauman, unpublished results.

(29) (a) J. P. Collman, R. G. Finke, J. N. Cawse, and J. I. Brauman, unpublished results; (b) J. P. Collman, J. N. Cawse, and J. I. Brauman, *J. Am. Chem. Soc.*, **94**, 5905 (1972).

(30) W. F. Edgell, M. T. Yang, and N. Koitzumi, *J. Am. Chem. Soc.*, **87**, 2563 (1965).

(31) M. Y. Darensbourg, D. J. Darensbourg, D. Burns, and D. A. Drew, *J. Am. Chem. Soc.*, **98**, 3127 (1976).

(32) The total conductance is given by[27]

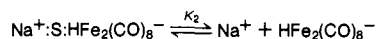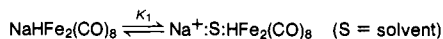$$\Lambda = \Lambda_0 \alpha + \lambda_0 \alpha_3$$

where Λ_0 and λ_0 are the molar conductivities at infinite dilution of dissociated NaHFe₂(CO)₈ and [Na⁺HFe₂(CO)₈⁻]Na⁺]⁺ plus [HFe₂(CO)₈⁻(Na⁺)HFe₂(CO)₈⁻]⁻ triple ions, respectively. Also, α is the degree of dissociation of NaHFe₂(CO)₈ while α_3 is the degree of *association* of the triple ions. For conditions where few triple ions and dissociated ions are formed relative to ion pairs (i.e., α and $\alpha_3 \ll 1$), Λ is given by (C = the initial [NaHFe₂(CO)₈])

$$\Lambda = \Lambda_0(K_0/C)^{1/2} + \lambda_0(CK_0)^{1/2}/K_{TO} \text{ (for } \alpha, \alpha_3 \ll 1)$$

Multiplying this equation by $C^{1/2}$ gives

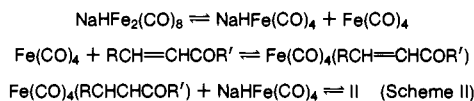$$\Lambda C^{1/2} = \Lambda_0(K_0)^{1/2} + \lambda_0(C)(K_0)^{1/2}/K_{TO}$$

Thus from a plot of $\Lambda C^{1/2}$ vs. C given the values of Λ_0 and λ_0, K_{TO} and K_0 can be determined. Order of magnitude values of K_{TO} and K_0 have been determined by this method using the $\Lambda C^{1/2}$ vs. C data near C = 10⁻² M, where a posteriori calculations show α and $\alpha_3 \lesssim 0.2$. A value of Λ_0 equal to 0.09 mho/(M cm), and the usual assumption,[27] $\lambda_0 = \frac{1}{3} \Lambda_0$, have been used. It should be noted that this treatment makes the usual but untested assumption that the dissociation constant, K_{TO}, is the same for positive and negative triple ions. Also, K_0 and K_{TO} are composite equilibrium constants because of the presence of solvent-separated ion pairs. For example, $K_0 = K_1 K_2/(1 + K_1)$ where

$$\text{NaHFe}_2(\text{CO})_8 \underset{}{\overset{K_1}{\rightleftharpoons}} \text{Na}^+ :S: \text{HFe}_2(\text{CO})_8 \quad (S = \text{solvent})$$

$$\text{Na}^+ :S: \text{HFe}_2(\text{CO})_8^- \underset{}{\overset{K_2}{\rightleftharpoons}} \text{Na}^+ + \text{HFe}_2(\text{CO})_8^-$$

(33) D. F. Shriver and Sr. Agnes Alich, *Coord. Chem. Rev.*, **8**, 15 (1972).

(34) (a) M. Szwarc, Ed., "Ions and Ion Pairs in Organic Reactions", Vol. 1, Wiley-Interscience, New York, N.Y., 1972; (b) *ibid.*, Chapter 4; (c) *ibid.*, Vol. 2, 1974.

(35) J. P. Collman, R. G. Finke, J. N. Cawse, and J. I. Brauman, *J. Am. Chem. Soc.*, **99**, 2515 (1977).

(36) For 0.2 M *trans*-CH₃CH=CHCO₂Et, 0.2 M NaHFe₂(CO)₈, and 0.12 M HOAc the measured yields were 0.44 equiv CH₃CH=CHCO₂Et consumed and 0.52 equiv of CH₃CH₂CH₂CO₂Et and 0.57 equiv of NaHFe₃(CO)₁₁ formed. In a separate experiment, Fe(CO)₅ (43%) was observed in GLC.

(37) (a) J. P. Collman and W. O. Siegl, unpublished results. (b) A variety of RFe(CO)₄⁻ compounds, including [Fe(CO)₄CH₂CO₂Et]⁻, have been previously isolated as their PPN⁺ salts: W. O. Siegl and J. P. Collman, *J. Am. Chem. Soc.*, **94**, 2516 (1972).

(38) For the reaction of 0.20 M NaHFe₂(CO)₈ and 0.20 M ethyl crotonate in THF-d₈ (entry 6, Table V), after all the NaHFe₂(CO)₈ (1 equiv) had been

consumed, NMR analysis showed 0.6 equiv of Na⁺[CH₃CH₂CH(Fe-(CO)₄)CO₂Et]⁻, which was converted to 0.6 equiv of CH₃CH₂CH₂CO₂Et by acid. Analysis of the products for the reaction between 0.10 M NaHFe₂(CO)₈ and 0.40 M ethyl crotonate showed 0.28 ± 0.04 equiv of Fe(CO)₅ and 0.24 ± 0.03 equiv of NaHFe₃(CO)₁₁. After acid quench, 0.35 ± 0.05 equiv of NaHFe₃(CO)₁₁ was found, along with 0.57 equiv of ethyl butyrate, 0.32 equiv of *cis*-ethyl crotonate, and 2.71 equiv of *trans*-ethyl crotonate. The increase in NaHFe₃(CO)₁₁ after acid quench suggests that 0.1 equiv of Na₂Fe₃(CO)₁₁ was present before the HOAc addition (separately, (PPN)₂Fe₃(CO)₁₁ was separated in 5% yield from 0.1 M NaHFe₂(CO)₈ and 0.1 M ethyl acrylate). These yields account for 98% of the CO initially present and 99% of the iron. No Fe₃(CO)₁₂ was observed.

(39) For pseudo-first-order reactions with NaHFe₂(CO)₈ in excess and no HOAc, ln (R_0/R_i) vs. time plots (R = [*trans*-CH₃CH=CHCO₂Et]) curved up with time indicating that the reaction went faster with time than expected for a first-order reaction. Linear plots for orders X (X = 0.4–0.6) of [R_i]⁻ˣ⁺¹ vs. time were obtained under these conditions. However, these reactions are clearly first order [*trans*-CH₃CH=CHCO₂Et] (Figure 8) and not 0.4–0.6 order. These deviations from linearity are not understood at the present time. Excess HOAc has the opposite effect, causing ln (R_0/R_i) vs. time plots to curve down since [NaHFe₂(CO)₈] is not constant but is decreasing due to an HOAc-dependent decomposition mechanism. Thus it appears that the ln (R_0/R_i) vs. time plots for NaHFe₂(CO)₈ in excess with 0.088 M HOAc present are fortuitously linear within experimental error (Figure 7) owing to these opposing effects.

(40) J. Kwiatek, *Catal. Rev.*, **1**, 37 (1967).

(41) The stereochemistry of overall hydrogen additions to α,β-unsaturated carbonyl compounds can be determined by the use of maleic and fumaric acids or their esters, and deuterium. IR analysis can be used to distinguish between the resulting meso vs. *dl* products.[42] The isolated dimethyl succinate product from the reaction of 0.08 M NaDFe₂(CO)₈, 0.07 M dimethyl maleate, and 0.16 M DOAc gave an IR indistinguishable from a similar reaction using dimethyl fumarate. However, the rapid maleate to fumarate isomerization and the formation of dideuterio-CH₃O₂CCD₂CX₂CO₂CH₃ (X = H or D) complicate the interpretation of these results.

(42) C. R. Childs, Jr., and K. Bloch, *J. Org. Chem.*, **26**, 1630 (1961).

(43) The activation parameters are consistent with this reaction being CO(gas) → CO(solution); $\Delta H^{\ddagger}$ = 6.0 ± 0.2 kcal/mol and $\Delta S^{\ddagger}$ = 56 ± 5 eu (standard state = M/s⁻¹), determined at five temperatures in the range of 4.6–50.2 °C. Error bars represent one standard deviation from the least-squares analysis.

(44) The ¹³CO ¹³C NMR resonance peak height of NaHFe₂(CO)₈ using exactly the same ¹³C NMR parameters (e.g., acquisition time, number of transients, etc.) was reproducible to within ±10%; thus a 20% or more increase in the ¹³C NMR resonance corresponding to ≥1.1% CO exchange would have been easily detectable.

(45) The ¹³C CO resonance of iron carbonyls is relatively insensitive to the nature of the iron compound but sensitive to the oxidation state of iron. For example, the ¹³C CO resonances of 0.1 M NaHFe₂(CO)₈ and 0.5 M NaHFe(CO)₄ in THF and 0.5 M Na₂Fe(CO)₄ in *N*-methylpyrrolidinone occur at 222, 223, and 232 ppm downfield from Me₄Si, respectively, at ambient temperature.

(46) The actual ratios observed by ¹H NMR were for every 3.0 equiv of NaHFe₂(CO)₈ consumed, 2.0 equiv of NaHFe(CO)₄, 1.0 equiv of NaHFe₃(CO)₁₁, and 1.0 equiv of Fe(CO)₅ (GLC analysis) were produced.

(47) For every 1.0 equiv of NaHFe₂(CO)₈ that was consumed, 0.50 equiv of NaHFe₃(CO)₁₁ and 0.50 equiv of Fe(CO)₅ were observed within a 10% error. The presence of H₂ was verified by GLC analysis.

(48) (a) Slurries of Na₂Fe(CO)₄-1.5dioxane and HOAc in dioxane slowly turn red with H₂ evolution. After centrifugation, IR analysis shows that NaHFe₃(CO)₁₁ is present. However, this supernatant has a *trans*-CH₃CH=CHCO₂Et reducing power of <10⁻³ M. Protonation of a slurry of isolated Na₂Fe₂(CO)₈ in dioxane with HOAc leads to rapid H₂ evolution to yield a red solution which contains NaHFe₃(CO)₁₁ and NaHFe(CO)₄ but has low reducing power. Reductions in dioxane using Na₂Fe(CO)₄-1.5dioxane, Fe(CO)₅, and HOAc are subject to severe CO inhibition which is removed by flushing with nitrogen. (b) Initial reductions by NaHFe(CO)₄ or its decomposition could yield Fe(CO)₄, which could then combine with NaHFe(CO)₄ yielding NaHFe₂(CO)₈. Since NaHFe₂(CO)₈ reductions appear to give Fe(CO)₄ as an iron by-product, a steady-state concentration of NaHFe₂(CO)₈ would then be established.

(49) T. Mitsudo, Y. Watanabe, M. Yamashita, and Y. Takegami, *Chem. Lett.*, 1385 (1974). They report that 1 atm of CO "dramatically" supresses this reaction.

(50) The ¹³C CO resonance of NaHFe(CO)₄ was enhanced 65 ± 16%.

(51) R. Noyori, I. Umeda, and T. Ishigami, *J. Org. Chem.*, **37**, 1542 (1972).

(52) R. W. Goetz and M. Orchin, *J. Am. Chem. Soc.*, **85**, 2782 (1963).

(53) J. Kwiatek, *Catal. Rev.*, **1**, 37 (1967).

(54) (a) R. K. Boeckman, Jr., and R. Michalak, *J. Am. Chem. Soc.*, **96**, 1623 (1974); (b) S. Masamune, G. S. Bates, and P. E. Georghiou, *ibid.*, **96**, 3686 (1974).

(55) (a) A. J. Birch and K. A. M. Walker, *J. Chem. Soc. C*, 1894 (1966); (b) R. E. Harmon, J. L. Parsons, D. W. Cooke, S. K. Gupta, and J.Schoolenberg, *J. Org. Chem.*, **34**, 3684 (1969); (c) J. F. Biellmann and M. J. Jung, *J. Am. Chem. Soc.*, **90**, 1673 (1968); (d) F. H. Jardine and G. Wilkinson, *J. Chem. Soc. C*, 270 (1967); (e) J. P. Candlin and A. R. Oldham, *Discuss. Faraday Soc.*, **46**, 60, 92 (1968).

(56) (a) I. Ojima, "Organotransition Metal Chemistry", Y. Ishii and M. Tsutsui, Ed., Plenum Press, New York, N.Y., 1975, p 255; (b) I. Ojima, M. Kumagai, and Y. Nagai, *Tetrahedron Lett.*, 4005 (1974); (c) I. Ojima and T. Kogure, *ibid.*, 5035 (1972).

(57) (a) T. Kitamura, N. Sakamoto, and T. Joh, *Chem. Lett.*, 379 (1973); (b) T. Kitamura, T. Joh, and N. Hagihara, *ibid.*, 203 (1975).

(58) Y. Sasson and J. Blum, *J. Org. Chem.*, **40**, 1887 (1975).

(59) C. E. Castro, R. D. Stephens, and S. Mojé, *J. Am. Chem. Soc.*, **88**, 4964 (1966).

(60) S. B. Kadin, *J. Org. Chem.*, **31**, 620 (1966).
(61) S. K. Malhortra, D. F. Meakly, and F. Johnson, *J. Am. Chem. Soc.*, **89**, 2794 (1967).
(62) (a) R. L. Augustine, *J. Org. Chem.*, **23**, 1853 (1958); (b) R. L. Augustine, "Catalytic Hydrogenation", Marcel Dekker, New York, N.Y., 1965; (c) *ibid.*, p 60.
(63) (a) M. Smith in "Reduction", R. L. Augustine, Ed., Marcel Dekker, New York, N.Y., 1968, pp 95–170; (b) A. J. Birch and H. Smith, *Q. Rev., Chem. Soc.*, **12**, 17 (1958); (c) H. O. House, "Modern Synthetic Reactions", W. A. Benjamin, Menlo Park, Calif., 1972, pp 173–181; (d) C. Djerassi, Ed., "Steroid Reactions", Holden-Day, San Francisco, Calif., 1963, pp 267–288, 299–325; (e) K. W. Bowers, R. W. Giese, J. Grimsaw, H. O. House, N. H. Kolodny, K. Kronberger, and D. K. Roe, *J. Am. Chem. Soc.*, **92**, 2783 (1970); (f) H. O. House, R. W. Giese, K. Kronberger, J. P. Kaplan, and J. F. Simeone, *ibid.*, **92**, 2800 (1970).
(64) J. G. St. C. Buchanan and P. D. Woodgate, *Q. Rev., Chem. Soc.*, **23**, 522 (1969).
(65) These results have been verified in our laboratories.
(66) For example, consider the following mechanism:

$$NaHFe_2(CO)_8 \rightleftharpoons NaHFe(CO)_4 + Fe(CO)_4$$

$$Fe(CO)_4 + RCH{=}CHCOR' \rightleftharpoons Fe(CO)_4(RCH{=}CHCOR')$$

$$Fe(CO)_4(RCHCHCOR') + NaHFe(CO)_4 \rightleftharpoons II \quad (Scheme\ II)$$

(67) E. Weiss, K. Stark, J. E. Lancaster, and H. D. Murdoch, *Helv. Chim. Acta*, **46**, 288 (1963).
(68) The rapid ^{13}CO exchange with $NaHFe(CO)_4$ could involve the hydride's trans effect,[69] since $NaRFe(CO)_4$ (R = acyl) gives only 5% ^{13}CO exchange in 22 h,[29a] and could also involve an ion pair catalyzed CO dissociation.
(69) J. E. Huheey, "Inorganic Chemistry: Principles of Structure and Reactivity", Harper and Row, New York, N.Y., 1972, p 423.
(70) E. L. Muetterties and G. D. Stucky, unpublished results. We thank Professor Muetterties and Professor Stucky for permission to cite this result.
(71) (a) For example, the iron–iron bond distances of 2.523 (1) Å in $Fe_2(CO)_9$ (three bridging CO's)[71b] and 2.787 (2) Å in $Fe_2(CO)_8^{2-}$ (no bridging groups),[25] respectively, support this conclusion. (b) F. A. Cotton and J. M. Troup, *J. Chem. Soc., Dalton Trans.*, 800 (1974).
(72) M. R. Churchill and S. W. Y. Chang, *Inorg. Chem.*, **13**, 2413 (1974).
(73) (a) B. R. James, "Homogeneous Hydrogenation", Wiley, New York, N.Y., 1973, pp 123–147; (b) J. Kwiatek, *Catal. Rev.*, **1**, 37 (1967); (c) L. M. Jackman, J. A. Hamilton, and J. M. Lawlor, *J. Am. Chem. Soc.*, **90**, 1914 (1968); (d) J. Halpern and L. Y. Wong, *ibid.*, **90**, 6665 (1968).
(74) The radicals we have observed by ESR increase or remain at approximately the same concentration during reduction reactions. Thus these radicals are stable—present even long after the reaction is complete—and appear to be small concentrations of radical *products*, not reactive intermediates. However, further studies will be required to determine whether or not these ESR signals are due to $HFe(CO)_4 \cdot$ and $Fe(CO)_4^- \cdot$, and whether or not these radicals are responsible for the cis $\rightleftharpoons$ trans olefin isomerizations and allylic carbon–hydrogen bond activations that we have observed.
(75) One possible structure is obtained by the formation of a (ketonic) bridging carbonyl without a metal–metal bond (a "metal migration" as previously suggested by Poë[10b]). Kinetic evidence for the existence of some type of intermediate (thought to be a bridging carbonyl without a metal–metal bond, analogous to D) exists in other systems.[76] Also D is consistent with our

(21)
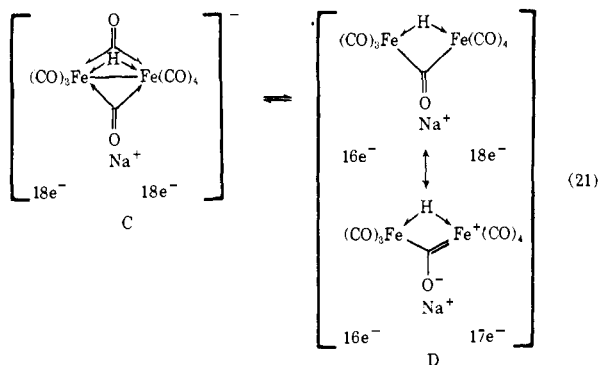
finding that tight-ion pairs are more reactive in these reductions and that the Na^+ cation binds preferentially to the bridging carbonyls. Caution should be exercised, however, as to what structures like D really mean. Cotton[77a] has suggested that bridging carbonyls cannot exist in the absence of a

metal–metal bond. He[77b] and others[77c] have pointed out that bridging carbonyls are not "ketonic bridges" but are, rather, best described as three-center, two-electron bonds (as we have indicated in C and D by the use of singly headed arrows). This view is consistent with the different bond angles observed in the two systems. For bridging carbonyls, the M–C–M angle[77c] is about 80° while the corresponding angle in organic carbonyl compounds is about 120°.
(76) (a) P. F. Barrett and K. K. W. Sun, *Can. J. Chem.*, **48**, 3300 (1970); (b) B. F. Barrett and W. J. Jacobs, *ibid.*, **50**, 972 (1972); (c) However, note that the Barrett work[76a,b] has been questioned by others[76d] and that these reactions are greatly enhanced by light; (d) J. D. Cotton and A. M. Trewin, *J. Organomet. Chem.*, **117**, C7 (1976).
(77) (a) F. A. Cotton and D. L. Hunter, *Inorg. Chem.*, **13**, 2044 (1974); (b) F. A. Cotton, *Prog. Inorg. Chem.*, **21**, 1 (1976); (c) P. S. Braterman, *Struct. Bonding (Berlin)*, **10**, 57 (1972).
(78) (a) The inverse isotope effect requires that $k_{-1} > k_2$, $k_3[HOAC]$ and that the concentration of II be small. The isotope effect arises from zero point energy differences between C–H and Fe–H vs. C–D and Fe–D vibrations. Using $Ru_4H_4(CO)_{12}$ as a model (S. A. R. Knox, J. W. Koepke, M. A. Andrews, and H. D. Kaesz, *J. Am. Chem. Soc.*, **97**, 3942 (1975)), bands are observed at 1585, 1442 (Raman), and 1290 cm^{-1} which shift to 1153, 1019, and 909 cm^{-1} in the deuteride. The 1019-cm^{-1} value was calculated assuming that the 1442-cm^{-1} band will shift by $1/\sqrt{2}$. For the alkyl intermediate, chloroform was used as a model. The chloroform C–H bond shows a stretching vibration at 3019 cm^{-1} and a twofold degenerate bending vibration at 1259 cm^{-1}. These values are shifted to 2256 and 908 cm^{-1}, respectively, in $CDCl_3$ (see R. W. Alder, R. Baker, and J. M. Brown, "Mechanisms in Organic Chemistry", Wiley-Interscience, New York, N.Y., 1971, p 15). These values give $K_D/K_H \approx 2$. While these calculations are not intended to be definitive, they do show that a preequilibrium of the type I $\rightleftharpoons$ II will account for the observed isotope effect. (b) Although it has been argued[79a] that hydrogen transfer for an extremely endothermic, productlike transition state could give an inverse isotope effect, others[79b] have concluded that no authentic examples of this exist.
(79) (a) L. Melander, *Acta Chem. Scand.*, **25**, 3821 (1971); (b) R. P. Bell, *Chem. Soc. Rev.*, **3**, 513 (1974).
(80) M. Poliakoff and J. J. Turner, *J. Chem. Soc., Dalton Trans.*, 2276 (1974).
(81) The product, $Fe(CO)_3L_2$, is often observed[82] when one would naively expect only $Fe(CO)_4L$. The following pathway will account for $Fe(CO)_3L_2$ formation.[83]
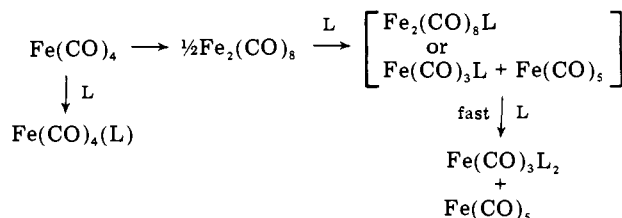
Others have also proposed that $Fe(CO)_4$ dimerization may be involved. I. Fischler, K. H. Idenbrand, and E. K. Von Gustorf, *Angew. Chem.*, **87**, 35 (1975).
(82) G. Gardaci, *Inorg. Chem.*, **13**, 368 (1974).
(83) The formation of $Fe(CO)_3L_2$ cannot be accounted for by the very slow reaction, $Fe(CO)_4L + L \rightarrow Fe(CO)_3L_2 + CO$ (rate = $k[Fe(CO)_4L]$; $k = 2.7 \times 10^{-4}$ s^{-1} at 179 °C in decalin): E. E. Siefert and R. J. Angelici, *J. Organomet. Chem.*, **8**, 374 (1967).
(84) W. G. Dauben, G. W. Shaffer, and N. D. Vietmeyer, *J. Org. Chem.*, **33**, 4060 (1968).
(85) J. C. Fairlie, G. L. Hodgson, and T. Money, *J. Chem. Soc., Perkin Trans. 1*, 2109 (1973).
(86) J. Colonge, J. Dreux, and M. Thiers, *C.R. Acad. Sci.*, **243**, 1425 (1958).
(87) C. C. Price and J. M. Judge, *Org. Synth.*, **45**, 22 (1966).
(88) R. L. Augustine and J. A. Caputo, "Organic Syntheses", Collect. Vol. V, Wiley, New York, N.Y., 1973, p 869.
(89) R. G. Komoto, Ph.D. Thesis, Stanford University, Stanford, Calif., 1974.
(90) J. N. Cawse, Ph.D. Thesis, Stanford University, Stanford, Calif., 1973.
(91) R. M. Izatt, B. L. Haymore, J. S. Bradshaw, and J. J. Christensen, *Inorg. Chem.*, **14**, 3132 (1975).
(92) R. Madon, Ph.D. Thesis, Stanford University, Stanford, Calif., 1974.
(93) W. F. Edgell, M. T. Yang, B. J. Bulkin, R. Bayer, and N. O. Koizumi, *J. Am. Chem. Soc.*, **87**, 3080 (1965).
(94) I. Wender and P. Pino, "Organic Synthesis via Metal Carbonyls", Wiley-Interscience, New York, N.Y., 1968, p 121.